

Half-Century Journey from Synthetic Organic Chemistry to Mathematical Stereochemistry through Chemoinformatics

SHINSAKU FUJITA

Shonan Institute of Chemoinformatics and Mathematical Chemistry, Kaneko 479-7
Ooimachi, Ashigara-Kami-Gun, Kanagawa-Ken, 258-0019 Japan

Correspondence should be addressed to shinsaku_fujita@nifty.com

Received 10 October 2015; Accepted 12 October 2015

ACADEMIC EDITOR: ALI REZA ASHRAFI

ABSTRACT My half-century journey started from synthetic organic chemistry. During the first stage of my journey, my interest in stereochemistry was initiated through the investigation on the participation of steric effects in reactive intermediates, cyclophanes, strained heterocycles, and organic compounds for photography. In chemoinformatics as the next stage of the journey, I proposed the concept of imaginary transition structures (ITSs) as computer-oriented representation of organic reactions. My interest was stimulated to attack combinatorial enumeration through the investigation on enumeration of subgraphs of ITSs. Stereochemistry and combinatorial enumeration was combined in my interest, so that I reached mathematical stereochemistry as the final stage of my journey. Fujita's unit-subduced-cycle-index (USCI) approach, Fujita's prolignand method, and Fujita's stereoisogram approach were developed, so as to integrate van't Hoff's way (asymmetry, stereogenicity) and Le Bel's way (dissymmetry, chirality), which caused continuous confusion in the history of stereochemistry.

KEYWORDS sphericity, combinatorial enumeration, stereoisogram, stereochemistry.

1. INTRODUCTION

I started my research career as a synthetic organic chemist in 1965 (a half century ago), when I joined the research group of Prof. Hitosi Nozaki, Kyoto University. I conducted experimental works on regioselective reactions of nitrenes [1] under the guidance of late Prof. Hidemasa Takaya (Kyoto University; at that time, a doctor-course student) and Prof. Ryoji Noyori (Nagoya University, the Nobel laureate in chemistry, 2001; at that time, a research instructor). In the same laboratory room, I had a fortunate opportunity to see the initial event of homogeneous asymmetric synthesis [2], by which Prof. Noyori was later

awarded the Nobel prize for chemistry, 2001 [3]. The event strongly impressed me with the importance of stereochemistry in the R&D on synthetic organic chemistry.

During a half century, I changed my positions three times: Kyoto University (1968–1972), Fuji Photo Film Co. Ltd. (1972–1997), and Kyoto Institute of Technology (1997–2007). In 2007, I have started Shonan Institute of Chemoinformatics and Mathematical Chemistry as a private laboratory. Although my research interests have shifted among synthetic organic chemistry, chemoinformatics, and mathematical stereochemistry, the first impression concerning the importance of stereochemistry remains unchanged through the half century.

The conventional stereochemistry for supporting synthetic organic chemistry was restricted to a qualitative phase, which had no sufficient mathematical formulations. My studies on synthetic organic chemistry demonstrated the participation of steric effects in reactive intermediates (such as nitrenes), cyclophanes, strained heterocycles, and organic compounds for photography. For example, steric hindrance avoids undesirable side reactions so as to enhance dye-releasing efficiency in instant color photography, as described in my book [4]. However, discussions on such steric effects were restricted to a qualitative phase.

The stereochemistry for supporting chemoinformatics had both qualitative and quantitative phases, which required theoretical foundations with mathematical formulations. In particular, enumeration and classification of organic compounds as three-dimensional (3D) entities inevitably required quantitative treatments with mathematical formulations. The struggle in chemoinformatics resulted in the concept of *imaginary transition structures* (ITSs), as summarized in my book [5]. However, this concept was still restricted to two-dimensional (2D) structures (graphs) and to the scope of the conventional stereochemistry without mathematical formulations.

It follows that my efforts focused on the development of new mathematical formulations, which enabled us to extend the conventional stereochemistry, to treat 3D structures effectively, and thereby to develop a new version of ITSs with 3D information. The first accomplishment was *the unit-subduced-cycle-index (USCI) approach*, which provided us with powerful methods of enumerating organic compounds in a symmetry-itemized fashion. The concept of *sphericities of orbits* was a key to treat 3D structures, as described in my book [6]. Fujita's USCI approach was further exploited to develop the concept of *mandalas*, which meets requirements of both chemists and mathematicians, as described in my book [7].

In comparison with symmetry-itemized enumeration, gross enumeration is convenient to get brief information on enumeration. Within the scope of 2D structures (graphs), Pólya's theorem has been adopted widely [8]. To accomplish gross enumeration of 3D structures, in contrast, I have developed *the proligand method*, as summarized in my

book [9]. The concept of *sphericities of orbits* for Fujita's USCI approach was transmuted into the concept of *sphericity of cycles* for Fujita's proligand method.

As an advanced theoretical foundations, I have developed the *stereoisogram approach*, where an *RS*-stereoisomeric group is defined by starting a point group [10, 11, 12]. Fujita's stereoisogram approach [13, 14, 15] provides theoretical foundations for rationalizing *R/S* descriptors of the Cahn-Ingold-Prelog (CIP) system [16, 17]. As summarized in my recent book [18], Fujita's stereoisogram approach brings about *Aufheben*, where van't Hoff's way (asymmetry, stereogenicity) [19, 20] and Le Bel's way (dissymmetry, chirality) [21, 22] are integrated by means of three attributes (chirality, *RS*-stereogenicity, and sclerality), which are defined by an *RS*-stereoisomeric group (quantitatively) or a stereoisogram as its diagrammatic expression (qualitatively).

In summary, stereochemistry has played a crucial role throughout the above-mentioned investigations, once mathematical concepts (especially group-theoretical and combinatorial concepts) have been combined with stereochemical concepts. Thus, I have pursued *mathematical stereochemistry* [18], which is an interdisciplinary field combining mathematics (in particular, group theory and combinatorial theory) and chemistry (in particular, organic stereochemistry). The present account is devoted to the introduction to my half-century journey from synthetic organic chemistry to mathematical stereochemistry through chemoinformatics.

2. JOURNEY IN SYNTHETIC ORGANIC CHEMISTRY

2.1. REACTIVE SPECIES AND STRAINED CYCLIC COMPOUNDS

From 1968 to 1972, I was a research instructor at Kyoto University, where I was engaged in investigation on stereoselective reactions of reactive species and on stereochemically-interesting compounds. As for stereoselective reactions, it was found that carbethoxynitrene **2** generated by the thermolysis (Δ) of ethyl azidoformate **1** attacks *trans*- and *cis*-propenylbenzenes **3** to produce the corresponding *trans*- and *cis*-aziridines **4** in a stereoselective fashion (Figure 1) [23]. Detailed reviews on nitrenes have appeared as chapters of books (in Japanese) [24, 25].

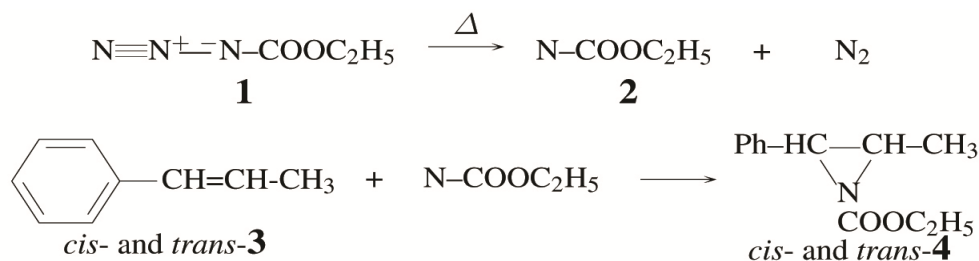


Figure 1. Stereoselective addition of carbethoxynitrene to *trans*- and *cis*-propenylbenzene.

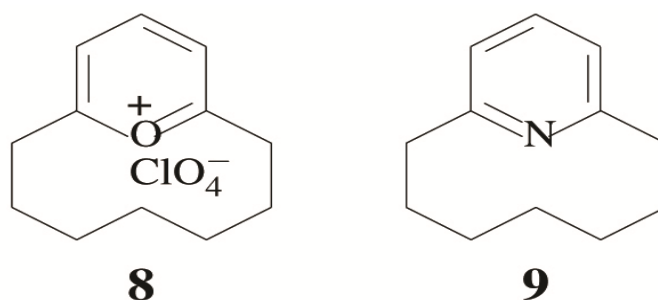


Figure 4. [7](2,6)pyrylophanium perchlorate and [7](2,6)Pyridinophane

As carbon analogs of [7](2,6)pyridinophanes (9 etc.), the nitrogen atom was replaced by a carbon atom to synthesize [7]metacyclophanes [32]. The heptamethylene chains of them were replaced by hexamethylene chains to produce [6]metacyclophanes [33, 34], where the steric effects of the hexamethylene chain on the steric strain of a benzene ring were compared with those of heptamethylene chain by means of nuclear-magnetic-resonance (NMR) technique.

2.3. ORGANIC CHEMISTRY OF PHOTOGRAPHY

In 1972, I moved to Ashigara Research Laboratories, Fuji Photo Film Co., Ltd., where I was first engaged in the R&D of organic compounds for instant color photography during about 15 years [35, 36].

Instant color photography adopted by Fuji is based on dye releasers, each of which is nondiffusible but releases a dye moiety in an unexposed area, as shown in Figure 5. From a viewpoint of patentability, we selected *o*-sulphonamidophenol as a dye-releasing moiety. Thus, a dye releaser **13**, which is initially immobile because of the presence of B (a ballast group), is oxidized by the action of an oxidized electron transfer agent **12** (ETAox) in an unexposed area. The resulting quinone monoimide **15** is hydrolyzed so as to release a diffusible dye **17**.

To adjust the redox potential of the *o*-sulphonamidophenol moiety of the dye releaser **13**, the substitution of an alkoxy substituent (as a ballast group) was found to be necessary in addition to an alkyl group. However, the mechanistic investigation of the hydrolysis process of **15** revealed that the substitution of an alkoxy substituent causes an undesirable side reaction [37, 38]. To avoid the undesirable side reaction, a sterically bulky group (e.g., a *tert*-butyl group) was introduced at the position adjacent to the alkoxy substituent.

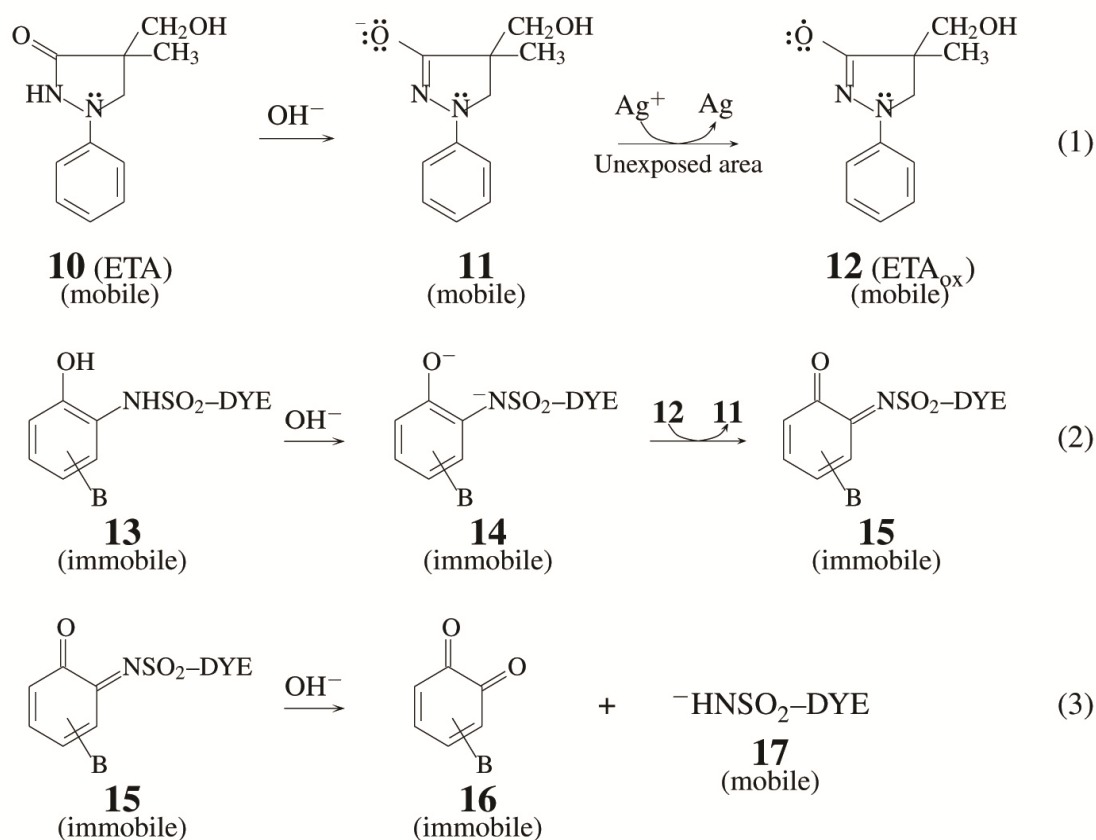


Figure 5. Mechanism of dye releasing in an unexposed area of instant color film (reversal type). The symbol B represents a ballast group for giving undiffusibility to the dye releaser. The symbol DYE is a dye moiety, so that DYE-SO₂NH⁻ represents a diffusible dye.

Finally, we selected an effective dye-releasing moiety shown in a shadowed box of Figure 6 [39], where the steric hindrance due to a *tert*-butyl group inhibits the undesired side reaction during the hydrolysis step. Moreover, a methoxyethoxy group in another shadowed box brought about the higher efficiency of dye releasing process [40]. The enhanced efficiency due to a methoxyethoxy group has been ascribed to the protonation of an imido nitrogen which would be assisted by a neighboring chelation of two oxygens [41, 42].

An instant color system requires three dye releasers according to the subtractive color reproduction, e.g., a cyan dye-releaser **18** [39], a magenta dye-releaser **19** [43], and a yellow dye-releaser **20** [39], as shown in Figure 6.

The R&D described above resulted in the FI-10 film, which was put on the market in 1981 under the system name “FOTORAMA” from Fuji Photo Film. Thereby, I (with Koichi Koyama and Shigetoshi Ono) was awarded Synthetic Organic Chemistry Award, Japan (1982). Our accomplishment was summarized as account articles [44, 45]. Later, I

published a book entitled “Organic Chemistry of Photography” [4], Chapters 15–20 of which dealt with the R&D of organic compounds for instant color photography.

3. JOURNEY IN CHEMOINFORMATICS

3.1. MOTIVATION GIVEN IN THE EDITORIAL COMMITTEE OF A JOURNAL

At the final stage of the project of developing dye releasers for instant color photography, I served as a member of the editorial committee of *Yuki Gosei Kagaku Kyokai-Shi (Journal of Synthetic Organic Chemistry, Japan)* during 1979–1982.

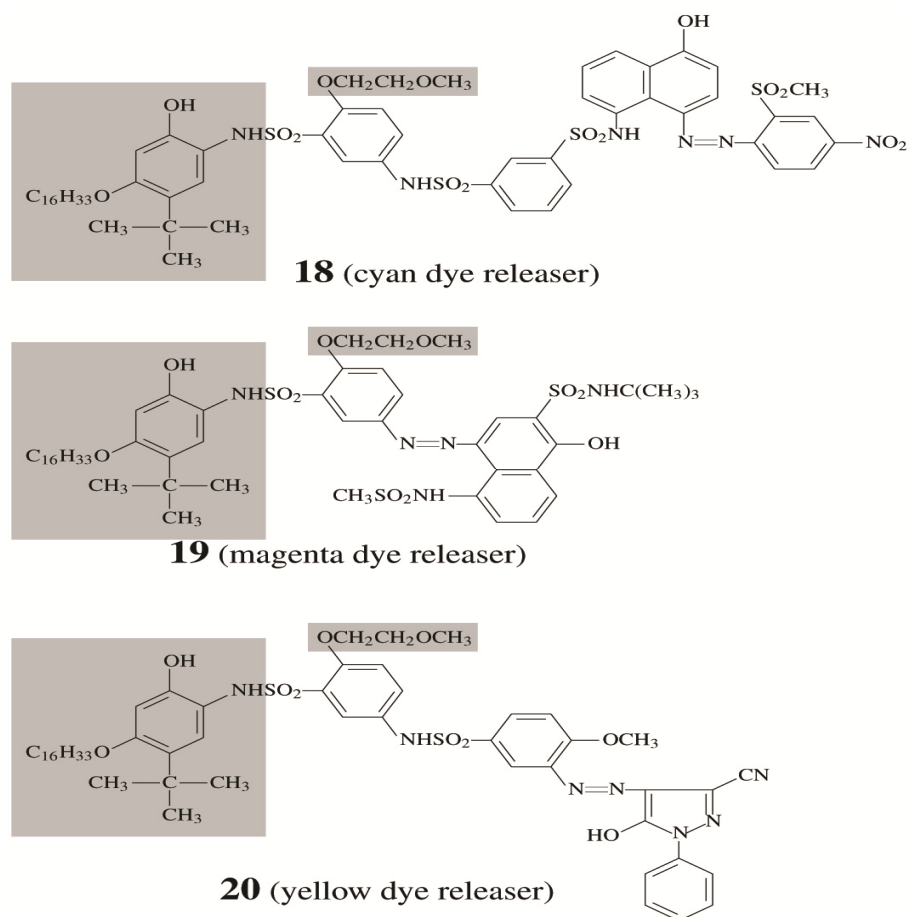


Figure 6. Dye releasers for instant color photography. The shadowed box indicates a common dye-releasing moiety.

The journal had a long-term series named “New Syntheses”, which appears in every issue even now. Because syntheses abstracted in the series had not been classified into types of reactions at that time, the editorial committee decided to attach keywords of reaction types for the sake of easy retrieval. Then, the selection of keywords was assigned to me as a member of the committee. After a list of selected keywords was adopted by the committee, the application was started from the issue 8 of volume 38 (1980). Compare the previous format of the issue 7 with the renewed format of the issue 8 of the same volume, if your library stores *Yuki Gosei Kagaku Kyokai-Shi*. The renewed format of “New Syntheses” is still active even in the recent issues of volume 73 (2015).

During the process of selection, I became aware that such keywords of reaction types were not linked with moieties to be attacked. For example, a keyword ‘cyclization’ attached to an abstracted item ‘formation of oxazoles’ was silent about how a cyclic moiety (oxazole) was formed from starting compounds. Thereby, I was motivated to develop a new system for specifying both reaction types and attacked moieties in an integrated fashion.

3.2. PROPOSAL OF IMAGINARY TRANSITION STRUCTURES (ITSS)

After trials and errors during several years, I reached the concept of *imaginary transition structures* (ITSS). The construction of an ITS is illustrated in Figure 7, which represents an acid-catalyzed hydrolysis of ethyl acetate.

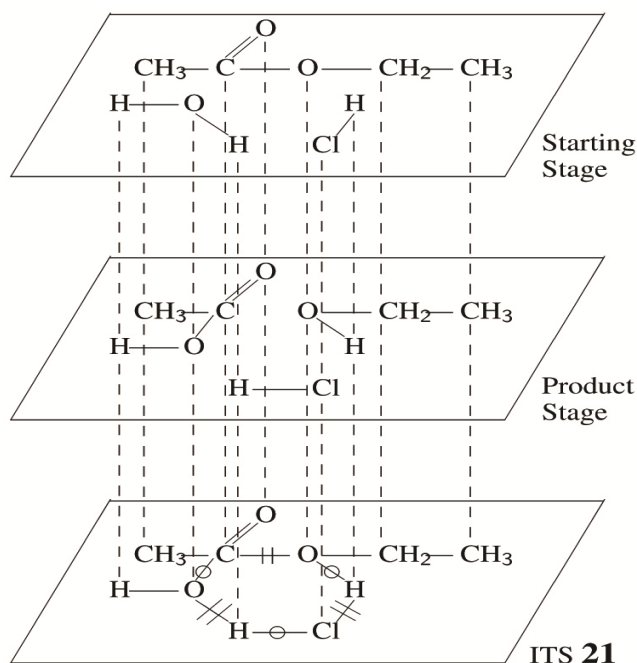


Figure 7. Construction of an imaginary transition structure (ITS) for representing an acidcatalyzed hydrolysis of ethyl acetate.

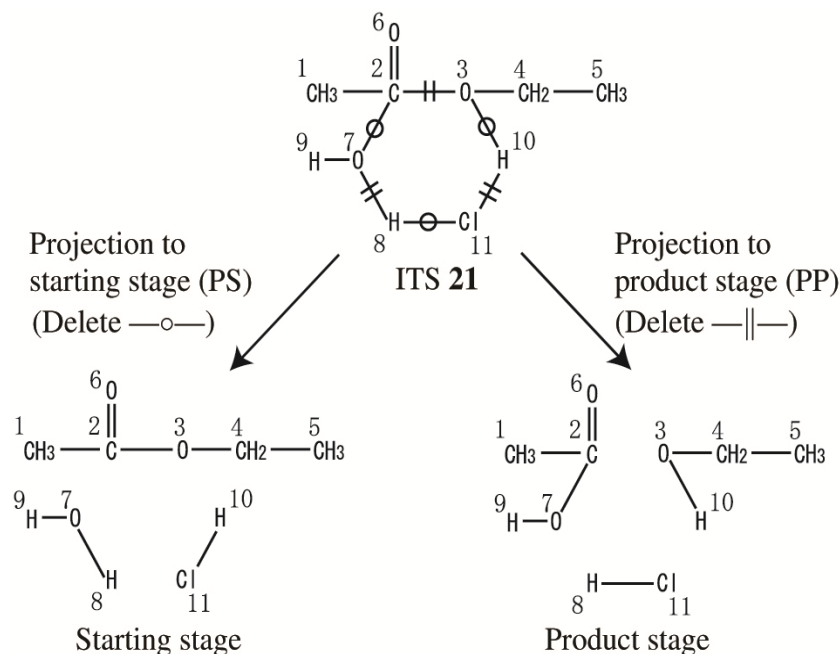


Figure 8. Projections to starting stage and to product stage.

The starting stage contains the structures of ethyl acetate, water, and hydrochloric acid, while the product stage contains those of acetic acid, ethanol, and hydrochloric acid. The two stages are superimposed to give an ITS **21**, which is characterized by three kinds of bonds, i.e., *in-bonds* (\square) for representing bonds formed, *out-bonds* (\parallel) for representing bonds cleaved, and *par-bonds* (—) for representing invariable bonds.

The resulting ITS **21** is capable of reproducing the starting stage by deleting in-bonds (projection to starting stage), as shown in the left branch of Figure 8 [46]. On the other hand, the product stage can be reproduced by deleting out-bonds (projection to product stage), as shown in the right branch of Figure 8 [46].

3.3. CONNECTION TABLES OF ITSS FOR COMPUTER STORAGE

The combination of inbonds, out-bonds, and par-bonds results in the appearance of fifteen bonds shown in Table 1 [46], because there are single bonds, double bonds, and/or triple bonds in starting and product stages.

The next task was the computer storage of ITSS. For this purpose, each of the fifteen bonds is represented by a pair of integers ($a\ b$) (Table 1), which is called a *complex bond number* (CBN). As found easily, the ($b = 0$)-column (the middle column) corresponds to usual single, double, and triple bonds, so that ITSS for representing organic reactions

contain usual structural formulas for representing organic compounds as a subcategory. In other words, an ITS is an extended structural formula having three kinds of bonds (in-bonds, out-bonds, and par-bonds), whereas usual structural formulas have par-bonds only.

Table 1. Fifteen imaginary bonds and complex bond numbers (CBNs)

Enrollment in local colleges, 2005.

$b =$	-3	-2	-1	0	+1	+2	+3
			\parallel	—	\ominus		
			(1 - 1)	(1 + 0)	(0 + 1)		
		\equiv	\parallel	\equiv	\ominus	\ominus	
		(2 - 2)	(2 - 1)	(2 + 0)	(1 + 1)	(0 + 2)	
	\equiv	\equiv	\parallel	\equiv	\ominus	\ominus	\ominus
	(3 - 3)	(3 - 2)	(3 - 1)	(3 + 0)	(2 + 1)	(1 + 2)	(0 + 3)

By using complex bond numbers, the data of an ITS is stored in the form of an *ITS connection table* [46], which is an extension of a connection table of a usual organic compound. For example, the data of the ITS **21** give an ITS connection table shown in Figure 9, where lines 8–19 store the information on the nodes of **21** and lines 20–31 store the information on the complex bond numbers of the respective bonds of **21**. For the numbering of nodes, see the ITS **21** shown in Figure 8.

Because ITSs put focus on covalent bonds, the original formulation of ITSs is not capable of treating formal charges appearing in nitro groups, sulfonic acids, and so on. For avoid this type of apparent difficulties, the concept of a *charge space* has been developed, where a three dimensional ITS with charges is recognized to be a synthesis space attached by a charge space [47].

The hydrolysis shown in Figure 7 has a multi-step mechanism from the starting stage to the product stage, if the participation of a proton dissociated from a hydrochloric acid is taken into consideration. To harmonize such a multi-step mechanism with the ITS **21**, the calculation of CBNs has been formulated. Thereby, a multi-step reaction (or a multi-step synthesis) can be treated within the scope of the ITS approach [48].

3.4. SUBSTRUCTURES (SUBGRAPHS) OF ITSs

Because ITSs for representing organic reactions can be regarded as an extension of structural formulas for representing organic compounds, there is much correspondence

between them. Most remarkable correspondence is concerned with their substructures (subgraphs). Just as substructures (subgraphs) of a structural formula provide information on compound types, substructures (subgraphs) of an ITS provide information on reaction types [49, 50].

00000380. iup											
I No 98640001-991022-01											
hydroxy-de-ethoxy lation											
hydroxy-de-alkoxy lation											
hydroxy-de-ethoxy -substitution											
hydroxy-de-alkoxy -substitution											
The hydrolysis of ethyl acetate											
11	0	IUPAC									
1	c	CH₃	10	20	0	0	0	0	0	0	0
2	c	C	35	20	0	0	0	0	0	0	0
3	0	0	60	20	0	0	0	0	0	0	0
4	c	CH₂	85	20	0	0	0	0	0	0	0
5	c	CH₃	110	20	0	0	0	0	0	0	0
6	0	0	35	45	0	0	0	0	0	0	0
7	0	0	25	10	0	0	0	0	0	0	0
8	H	H	35	0	0	0	0	0	0	0	0
9	H	H	10	10	0	0	0	0	0	0	0
10	H	H	70	10	0	0	0	0	0	0	0
11	c₁	c₁	60	0	0	0					
1	2	1	0	0	1	0	0	0	0		
2	3	1	-1	0	1	0	0	0	0		
2	6	2	0	0	1	0	0	0	0		
2	7	0	+1	0	1	0	0	0	0		
3	4	1	0	0	1	0	0	0	0		
3	10	0	+1	0	1	0	0	0	0		
4	5	1	0	0	1	0	0	0	0		
7	8	1	-1	0	1	0	0	0	0		
7	9	1	0	0	1	0	0	0	0		
8	11	0	+1	0	1	0	0	0	0		
10	11	1	-1	0	1	0	0	0	0		
999	0	0	0	0	0	0	0	0	0		

Figure 9. Connection table of ITS 21.

3.4.1. REACTION-CENTER GRAPHS, REACTION GRAPHS, AND BASIC REACTION GRAPHS

By extracting bonds with $b \neq 0$ of $(a\ b)$ (CBN) from an ITS, we obtain a substructure for representing a net reaction. To refer to the resulting substructure, the term *reaction-center graph* (RCG) has been coined [49, 50]. For example, the ITS 22, which represents a Diels-Alder reaction between cyclopentadiene and maleic anhydride, contains an RCG 26 (Figure 10). The other ITS 23 representing another Diels-Alder reaction gives an RCG 27. The RCGs 26 and 27 are graphic expressions of Diels-Alder reactions, which maintain the information on nodes (participant atoms).

By omitting the information on nodes from the RCG 26 (or 27), we obtain a subgraph 30 called a *reaction graph* (RG), in which each node is represented by a bullet symbol (\bullet) in an abstract fashion. The RG 30 is a more general expression of Diels-Alder reactions. As found in Figure 10, the RCG 28 (or 29) extracted from the ITS 24 (or 25) gives the corresponding RG 31, which represents a Claisen rearrangement in a more general fashion.

By omitting the information on par-bonds from the RG 30, we obtain a subgraph 32 called a *basic reaction graph* (BRG). The BRG 32 represents a net migration of electrons. As found in Figure 10, the BR 31 for representing Claisen rearrangements contains the same BRG 32. Moreover, the ITS 21 shown in Figure 8 contains the same BRG 32. It should be emphasized that the classification of organic reactions is replaced by graphic treatments of ITSs, which are illustrated from the ITS-column (left) to the BRG-column (right) of Figure 10.

3.4.2. REACTION STRINGS

As found in each of the ITSs, RCGs, RGs, and BRG collected in Figure 10, there appears a string in which in-bonds and out-bonds are linked alternately. Such a string is called a *reaction string*, which represents a shift of an electron pair. The number of reaction strings appearing in an ITS is a clue for classifying the ITS. Thereby, ITSs are classified into one-string reactions, two-string reactions, and so on.

In particular, two-string reactions in which the two reaction strings exhibit a spiro junction have been discussed as a remarkable category of reactions [51]. In addition, two-string reactions in which the two reaction strings exhibit a fused junction have been discussed as another remarkable category of reactions [52].

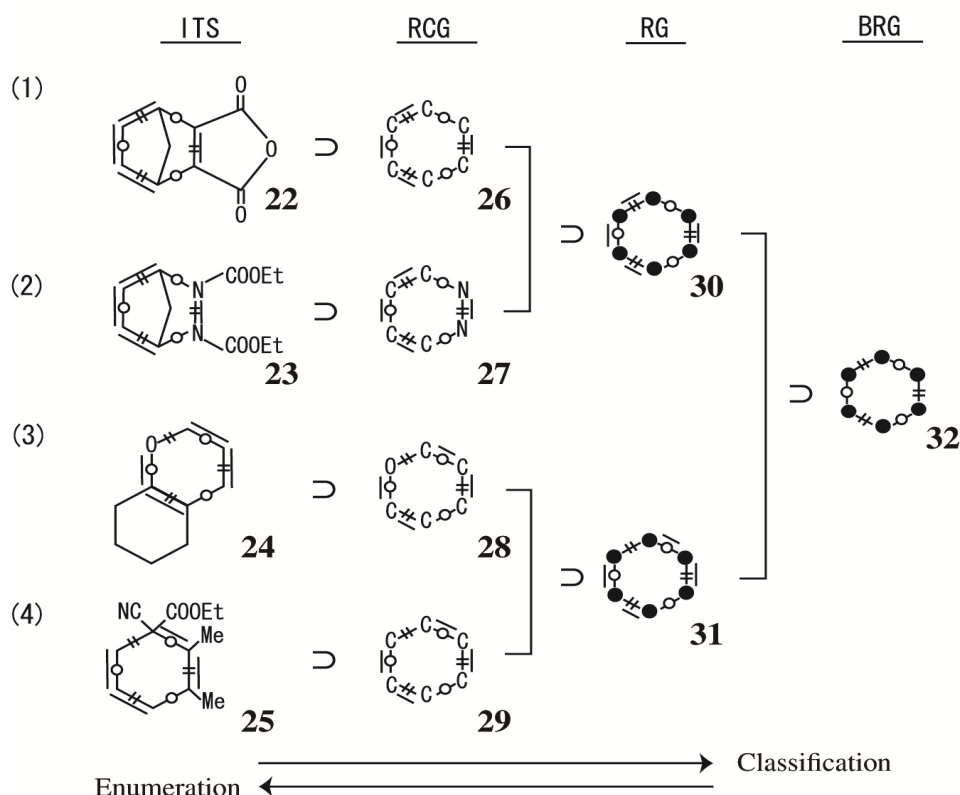


Figure 10. Six-membered imaginary transition structures (ITSs), reaction-center graphs (RCGs), and reaction graphs (RGs), which are related to a basic reaction graph (BRG).

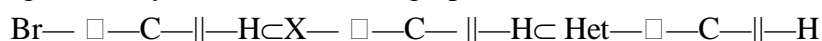
3.4.3. THREE-NODAL SUBGRAPHS AND FOUR-NODAL SUBGRAPHS

To retrieve substitution reactions, a *three-nodal subgraph* is defined as a substructure which consists of a reaction-center atom and adjacent atoms through an in-bond or an out-bond [53]. For example, the three-nodal subgraph $\text{O}-\square-\text{C}-\parallel-\text{O}$ is extracted from the ITS **21** (Figure 8) to show a substitution reaction. A more definite subgraph can be extracted from **21** by attaching additional information, e.g., $(\text{H})\text{O}-\square-\text{C}(=\text{O})-\parallel-\text{O}(\text{C})$ for the purpose of representing a hydrolysis of an ester.

In a similar way, a *four-nodal subgraph* is defined for the purpose of retrieving C—C bond formations, C—C bond cleavages, additions, and eliminations [53]. For example, the four-nodal subgraph $\text{Br}-\parallel-\text{C}-\square-\text{C}-\parallel-\text{Br}$ represents a C—C bond formation with debromination, while the four-nodal subgraph $\text{O}-\square-\text{C}-\parallel-\text{C}-\square-\text{O}$ represents a C—C bond cleavage.

A hierarchical classification can be accomplished by considering the classification of atoms which are contained in a three-nodal or four-nodal subgraph [54]. For example,

the hierarchy ‘bromine \subset halogen \subset electron-attracting atom’ ($\text{Br} \subset \text{X} \subset \text{Het}$) provides the following hierarchy of three-nodal subgraphs:



This result expresses the hierarchy ‘bromination \subset halogenation \subset oxidation’ graphically.

3.4.4. RING STRUCTURES IN ITSs

Among ring structures appearing in ITSs, *bridges of ring closure* (BC_n), *bridges of ring opening* (BO_n), and *bridges of rearrangement* (BR) are defined to retrieve ring closures, ring openings, and rearrangements, respectively [46].

The subscript n of BC_n (or BO_n) represents the number of bond formed (or cleaved) during the ring closure (or ring opening). For example, The ITS **22** (or **23**), the RCG **26** (or **27**), and the RG **30** are recognized to contain BC_2 ’s at the respective levels of categorization. A pair of BC_n and BO_n is called a *reaction pair*, which corresponds to a pair of forward and reverse reactions.

A bridge of rearrangement (BR) is a key of single-access perception of rearrangement reactions [55]. For example, the ITS **24** (or **25**), the RCG **28** (or **29**), and the RG **31** are recognized to contain BRs at the respective levels of categorization. These BRs indicate Claisen rearrangements.

Among all of the ring structures contained in an ITS, a minimum set of ring structures for specifying reactions is defined as *an essential set of essential rings* (ESER) [56]. An algorithm developed for the detection of an ESER in an ITS has been effective to the logical perception of ring-opening, ring-closure, and rearrangement reactions. The algorithm has been applied to the detection of an ESER in a usual structural formula [57].

3.4.5. CANONICAL NAMES OF ITSs

An algorithm for giving a canonical number and a canonical code to an ITS has been developed [58], where Morgan’s algorithm for giving a canonical numbering to a structural formula has been extended to meet the presence of three kinds of bonds.

An algorithm for giving a canonical number and a canonical code to an RCG extracted from an ITS has been developed [59], where there has appeared a novel approach to the linear coding of reaction types.

3.5. ENUMERATION OF REACTION GRAPHS AND REACTION-CENTER GRAPHS

The classification shown in Figure 10 has been accomplished by examining from the left to the right in the following order: ITS (e.g., **22**) \rightarrow RCG (e.g., **26**) \rightarrow RG (e.g., **30**) \rightarrow BRG (e.g., **32**). Let us examine the reverse order (right to left) in Figure 10. Then, the placement of four par-bonds on the edges of the BRG **32** generates an RG **30**; and the placement of

carbons on the nodes of the RG **30** generates an RCG **26**. As a result, the reverse order corresponds to the systematic method for enumerating RGs and RCGs.

Let us first enumerate RGs by starting from the BRG **32**, which belongs to a permutation group **D**₃. By applying Pólya's theorem [8] to the six edges of the BRG **32**, we obtain the following cycle index (CI):

$$Z(\mathbf{D}_3; s_d) = (1/6)(s_1^6 + 3s_1^2s_2^2 + 2s_3^2). \quad (4)$$

Suppose that m double par-bonds and n single par-bonds are placed on the six edges of **32**. The dummy variables x and y are used to count double par-bonds and single par-bonds, respectively. Thereby, the following ligand-inventory function is obtained:

$$s_d = 1 + x^d + y^d \quad (5)$$

where the top term 1 in the right-hand side represents no edge substitution. After Eq. 5 is introduced into Eq. 4, the resulting equation is expanded to give the following generating function:

$$\begin{aligned} G(x,y) &= Z(\mathbf{D}_3; 1+x^d+y^d) \\ &= (1/6)\{(1+x+y)^6 + 3(1+x+y)^2(1+x^2+x^2) + 2(1+x^3+x^3)^2\} \\ &= 1 + 2x + 2y + 4x^2 + 6xy + 4y^2 + 6x^3 + 12x^2y + 12xy^2 + 6y^3 + \\ &\quad 4x^4 + 12x^3y + x^6 + 2x^5y + 4x^4y^2 + 6x^3y^3 + 4x^2y^4 + 2xy^5 + y^6. \end{aligned} \quad (6)$$

where the coefficient of the term $x^m y^n$ represents the number of RGs with m double par-bonds and n single par-bonds. Six-membered reaction graphs with single parbonds ($m = 0, n = 0-6$) are depicted in Table 2, where the no.-of-RGs column collects the coefficients appearing in Eq. 6. The no.-of-RPs column of Table 2 collects the number of reaction pairs, where a pair of BC_n and BO_n (as well as an BR) is counted once in another calculation according to Pólya's theorem [60, 8].

This method is effective to accomplish systematic enumeration of organic reactions, e.g., even-membered RGs [49], odd-membered RGs [50], two-string RGs with spiro junction [51], and two-string RGs with fused junction [52].

Let us next enumerate RCGs by starting from an RG (**30** or **31**), where the six vertices accommodate a set of six atoms selected from carbon, nitrogen, and oxygen. In this case, the valence of each atom should be taken into consideration [61]. This type of enumeration with considering *obligatory minimum valences* (OMVs) has been conducted by using different ligand-inventory functions [62]. For OMVs of compound enumeration, see Chapter 14 of my book [6].

3.6. COMPUTER-RETRIEVAL SYSTEM BASED ON ITSS

3.6.1. APART FROM THE 'STRUCTURE—REACTION-TYPE' PARADIGM

The conventional description of organic reactions is a scheme in which the starting stage and the product stage are combined with an arrow, or a verbal description of the starting stage attached by a reaction type, e.g., 'the hydrolysis of ethyl acetate' [63]. This means that the conventional description suffers from the 'structure—reaction-type' paradigm, which is not necessarily suitable to computer manipulation [64]. As discussed in the preceding subsections, the concept of imaginary transition structures (ITSs) is capable of overcoming this paradigm. The total features of ITSs as a new computer-oriented representation has been discussed in review articles [65, 66].

3.6.2. DEVELOPMENT OF AN IN-HOUSE SYSTEM FORTUNITS

During 1986–1995, I was engaged in the development of an in-house system for retrieving organic reactions named FORTUNITS (Fuji Organic Reaction Treating Unity based on Imaginary Transition Structures). The FORTUNITS system was an integrated system composed of a subsystem of ITS registration, a subsystem of descriptive data, and a subsystem of retrieval system (running as a time-sharing system), as well as a subsystem of analyzing ITSs and a subsystem of analyzing compound structures (running as a batch system) [67, 68]. Several illustrations of computer displays have appeared in my review article [65], where in-bonds and out-bonds in ITSs are differentiated in the form of colored bonds.

3.7. PERSPECTIVES BROUGHT ABOUT BY THE CONCEPT OF ITSS

The ITS approach developed by Fujita stems from a principle that each organic reaction is represented by an ITS as a diagrammatic expression, which is recognized as a kind of structural formula. As a result, reaction types are ascribed to various substructures (subgraphs) contained in each ITS.

By applying the scheme $[ITS \rightarrow RCG \rightarrow RG \rightarrow BRG]$ according to Fujita's ITS approach, more abstract substructures (subgraphs) as hierarchical descriptors of organic reactions are successively extracted from each ITS (cf. Figure 10). The reverse scheme $[ITS \leftarrow RCG \leftarrow RG \leftarrow BRG]$, when combined with Pólya's theorem, gives a powerful methodology for enumerating organic reactions.

Moreover, the concept of ITSs provides a novel approach to the taxonomy of organic reactions. In other words, organic reactions are described systematically according to Fujita's ITS approach in a different way from classical descriptions in textbooks on

organic chemistry. The merits of ITSs have been summarized in my book on computer-oriented representation of organic reactions [5].

Table 2. Six-membered reaction graphs ($m = 0, n = 0 - 6$).

m	n	no. of		reaction graphs (RGs)
		RGs	RGs	
0	0	1	1	
0	1	2	1	
0	2	4	3	
0	3	6	3	
0	4	4	3	
0	5	2	1	
0	6	1	1	

3.8. EXCURSIVE JOURNEY TO $X^Y\text{MT}_E\text{X}$, $X^Y\text{M}$ NOTATION, AND $X^Y\text{MML}$

To continue my journey, I needed a writing tool for supporting both structural formulas and mathematical equations. Although the $\text{T}_E\text{X}/\text{L}^A\text{T}_E\text{X}$ system had already provided us with a satisfactory utility for writing mathematical equations, it lacked a utility for drawing structural formulas. So I decided to develop a utility for drawing structural formulas. The first version of $X^Y\text{MT}_E\text{X}$ was released in 1993 [69, 70]. Several improvements were added to enhance the feasibilities of $X^Y\text{MT}_E\text{X}$ [71, 72]. A book for introducing the $X^Y\text{MT}_E\text{X}$ system was published in 1997 [73]. The present version (Version 5.01) is available from

my homepage (<http://xymtex.com/>) with an on-line manual of 780 pages [74]. All of the structural formulas contained in this account article (except ITSs) have been drawn by X^YMT_EX Version 5.01. For example, see Figures 5 and 6.

The codes of the X^YMT_EX system can be regarded as a linear notation, which was brushed up into X^YM notations for electronic communication of structural formulas [75]. The X^YMML (X^YM Markup Language) was developed as a more advanced format (a markup language) [76, 77]. The X^YMJava system [78] and the X^YMML system [79] were developed as a WWW (World Wide Web) communication tool for publishing of structural formulas. The X^YMT_EX system was discussed comprehensively as a versatile tool for writing, submission, publication, and internet communication in chemistry [80] as well as for publishing interdisciplinary chemistry/mathematics books [81].

4. JOURNEY IN MATHEMATICAL STEREOCHEMISTRY

4.1. MOTIVATION GIVEN THROUGH THE DEVELOPMENT OF FUJITA'S ITS APPROACH IN CHEMOINFORMATICS

In Fujita's ITS approach, stereochemical data of organic reactions have been treated in the form of three-dimensional imaginary transition structures (3D ITSs) with charges [47]. However, during the investigation on enumeration of organic reactions according to the reverse scheme [ITS ← RCG ← RG ← BRG] (Figure 10), I became aware that Pólya's theorem [60, 8] is concerned with graphs (under the action of permutation groups), not with 3D structures (under the action of point groups). This feature of Pólya's theorem means insufficient applicability to 3D structures, which are essential to discuss stereochemistry.

The traditional foundations of modern stereochemistry, on the other hand, lack mathematical formulations of 3D structures. Although 3D structures are discussed by using point groups from a viewpoint of quantum chemistry [82], the discussions on 3D structures from a stereochemical viewpoint are restricted to qualitative phase [83]. For example, the conventional terms 'enantiotopic' [84] and 'stereoheterotopic' [85] cannot be applied to quantitative purposes such as combinatorial enumeration of 3D structures under the action of point groups.

As found in the preceding paragraphs, mathematical formulations of 3D structures require new items which provide the linkage between mathematics and stereochemistry, i.e., *mathematical stereochemistry* as an interdisciplinary field. This section is devoted to the introduction of Fujita's USCI approach [6, 7], Fujita's proligand method [9], Fujita's

stereoisogram approach [18], and related topics, as state-of-the-art embodiments of mathematical stereochemistry.

4.2. FUJITA'S UNIT-SUBDUCED-CYCLE-INDEX (USCI) APPROACH

Fujita's USCI (unit-subduced-cycle-index) approach puts stress on equivalence relationships and equivalence classes (frequently called *orbits*) [86, 87]. Each orbit is governed by a coset representation and by a sphericity index, so that a set of suborbits derived from the orbit is characterized by a product of such sphericity indices, which is called a *unit subduced cycle index with chirality fittingness* (USCI-CF) [6]. This exhibits a sharp contrast to the traditional foundations of stereochemistry, which make light of equivalence relationships and equivalence classes.

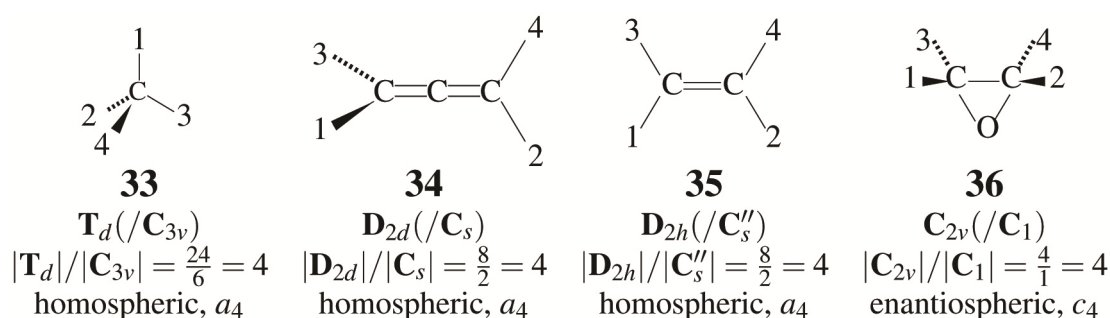


Figure 11. Representative stereoskeletons of ligancy 4. The four positions of each skeleton (numbered from 1 to 4) are equivalent to give a four-membered orbit governed by the cosetrepresentation shown below.

4.2.1. EQUIVALENCE CLASSES (ORBITS) AND COSET REPRESENTATIONS

In Fujita's USCI approach, an equivalence relationship is selected as a set of operations contained in a point group. The *proligand-promolecule model* is adopted for the purpose of avoiding effects of conformations [88]. A *proligand* is defined as an abstract ligand (group or substituent) which is characterized by chirality/achirality. A *promolecule* is defined as an abstract molecule which is derived by putting proligands on the substitution positions of a rigid *stereoskeleton* (or shortly, skeleton).

Such a rigid stereoskeleton is selected in accord with the purpose of our discussions. Representative stereoskeletons of ligancy 4 are shown in Figure 11: a tetrahedral skeleton **33** of the point group T_d (order, $|T_d| = 24$), an allene skeleton **34** of D_{2d} (order, $|D_{2d}| = 8$), an ethylene skeleton **35** of D_{2h} (order, $|D_{2h}| = 8$), and an oxirane skeleton **36** of C_{2v} (order, $|C_{2v}| = 4$).

The four positions of each stereoskeleton are equivalent under the action of the corresponding point group, so that they construct an equivalence class (orbit). Each orbit is

governed by a *coset representation* (CR) of the point group of a stereoskeleton at issue. For example, the four positions of a tetrahedral skeleton **33** construct an orbit governed by the CR, which is generated algebraically by considering a coset decomposition of a point group T_d by its subgroup C_{3v} , as shown in Table 3. The CR is a transitive permutation representation of degree 4 ($= |T_d|/|C_{3v}| = 24/6$). The symbol T_d/C_{3v} has been coined to denote the CR by Fujita [6], where it specifies the global symmetry T_d of the skeleton **33** as well as the local symmetry C_{3v} of each of the four positions. The resulting set of products of cycles for representing T_d/C_{3v} is isomorphic to the symmetric group of degree 4 ($S^{[4]}$) [6, 89].

In a similar way, the other stereoskeletons collected in Fig. 11 are characterized by the following coset representations (CRs): the CR D_{2d}/C_s for an allene skeleton **34** [88], the CR D_{2h}/C_s for an ethylene skeleton **35** [90], and the CR C_{2v}/C_1 for an oxirane skeleton **36** [91]. These CRs are isomorphic to the subgroups of the symmetric group of degree 4 ($S^{[4]}$).

4.2.2. SPHERICITIES AND CHIRALITY FITTINGNESS

Each orbit is categorized into either one of three kinds by examining the global symmetry G and the local symmetry G_i of the corresponding CR G/G_i [6]. As summarized in Table 4, there appear *enantiospheric*, *homospheric*, and *hemispheric* orbits according to the terms defined by Fujita [89]. These orbits are characterized by sphericity indices for orbits, i.e., a_d for d -membered homospheric orbits, c_d for d -membered enantiospheric orbits, and b_d for d -membered hemispheric orbits, where the subscript d represents the degree of the CR, which is calculated to be $d = |G|/|G_i|$.

The three kinds of sphericities control the modes of substitution on the positions of the respective orbits. The mode of substitution is called *chirality fittingness*, as illustrated in Figure 12 [6]. For example, the T_d/C_{3v} -orbit of the tetrahedral skeleton **33** is determined to be homospheric (Table 4), because both the global symmetry T_d and the local symmetry C_{3v} are achiral. Hence, the four positions of **33** accommodate four achiral proligands of the same kind (e.g., A) according to the chirality fittingness shown in Figure 12(a), where the global symmetry T_d maintains during this mode of substitution. This means that the resulting orbit of A's in the tetrahedral derivative CA_4 is governed by the CR T_d/C_{3v} . This mode of substitution is represented by the sphericity index a_4 assigned to T_d/C_{3v} , where the subscript 4 of a_4 is calculated to be $|T_d|/|C_{3v}| = 24/6 = 4$. The same discussions are effective to the homospheric orbits of the allene skeleton **34** and the ethylene skeleton **35**.

On the other hand, the C_{2v}/C_1 -orbit of the oxirane skeleton **36** is determined to be enantiospheric (Table 4), because the global symmetry C_{2v} is achiral, while the local symmetry C_1 is chiral. Hence, the four positions of **36** exhibit three modes of substitution to maintain the global symmetry C_{2v} , as shown in Figure 12(b). One mode is the accommodation of four achiral proligands of the same kind (e.g., A) according to the

chirality fittingness shown in the first diagram of Figure 12(b). The other mode is a compensated accommodation of two chiral proligands p 's (on the positions 1 and 4) and two chiral proligands \bar{p} 's (on the positions 2 and 3) according to the second diagram of Figure 12(b) (the third diagram degenerates onto the second diagram in this example), where a pair of p and \bar{p} is an enantiomeric pair in isolation. Note that one half of the C_{2v}/C_1 -orbit of the oxirane skeleton **36** (the positions 1 and 4) and the other half (positions 2 and 3) are separated to give two C_2/C_1 -orbits under an appropriate chiral condition, while they are compensated under an achiral condition so as to maintain the global achirality C_{2v} .

4.2.3. SUBDUCTION OF COSET REPRESENTATIONS AND USCI-CFs

The generation of derivatives from a given skeleton is treated by applying the concept of *subduction of coset representations* in Fujita's USCI approach [6]. The CR $G/(G_i)$ of a given skeleton is restricted to give a permutation representation of a subgroup G_j , where this process is called *a subduction of a coset representation* and denoted by the symbol $G/(G_i) \downarrow G_j$, as proposed by Fujita [92]. The permutation representation $G/(G_i) \downarrow G_j$ may be transitive or intransitive under the subgroup G_j , so that it can be treated algebraically to give a sum of coset representations, as discussed in Chapter 9 of [6]. Several results of subductions of coset representations have appeared in Appendix C of [6]. For example, $T_d/(C_{3v}) \downarrow C_{3v}$ gives the following result:

$$T_d/(C_{3v}) \downarrow C_{3v} = C_{3v}/(C_s) + C_{3v}/(C_{3v}), \quad (7)$$

which is calculated algebraically by using the mark table of T_d (Appendix A of [6]) and the inverse mark table of C_{3v} (Appendix B of [6]) according to the procedure described in Chapter 9 of [6].

The data of subduction of $T_d/(C_{3v})$ and related data (Table 5) are cited from a more recent report [93], which has discussed differences between point groups (e.g., T_d) and permutation groups (e.g., $S^{[4]}$, the symmetric group of degree 4). The subduction of Eq. 7 appears in the C_{3v} -row of Table 5.

Table 3. Coset representation $\mathbf{T}_d(/C_{3v})$.

Symmetry operation		CR	$\mathbf{T}_d(/C_{3v})$ as product of cycles	PSI(product sphericity indices)	Product of dummy variables
T	I	\sim	(1)(2)(3)(4)	b_1^4	s_1^4
	$C_{2(1)}$	\sim	(1 2)(3 4)	b_2^2	s_2^2
	$C_{2(2)}$	\sim	(1 4)(2 3)	b_2^2	s_2^2
	$C_{2(3)}$	\sim	(1 3)(2 4)	b_2^2	s_2^2
	$C_{3(1)}$	\sim	(1)(2 3 4)	$b_1 b_3$	$s_1 s_3$
	$C_{3(2)}$	\sim	(1 2 4)(3)	$b_1 b_3$	$s_1 s_3$
	$C_{3(3)}$	\sim	(1 4 3)(2)	$b_1 b_3$	$s_1 s_3$
	$C_{3(4)}$	\sim	(1 3 2)(4)	$b_1 b_3$	$s_1 s_3$
	$C_{3(1)}^2$	\sim	(1)(2 4 3)	$b_1 b_3$	$s_1 s_3$
	$C_{3(4)}^2$	\sim	(1 2 3)(4)	$b_1 b_3$	$s_1 s_3$
	$C_{3(3)}^2$	\sim	(1 4 2)(3)	$b_1 b_3$	$s_1 s_3$
	$C_{3(2)}^2$	\sim	(1 3 4)(2)	$b_1 b_3$	$s_1 s_3$

	Symmetry operation		CR T_d ($/C_{3v}$) as product of cycles	PSI(product sphericity indices)	Product of dummy variables
$T\sigma_{d(1)}$	$\sigma_{d(1)}$	\sim	$\overline{(1)(2\ 4)(3)}$	$a_1^2 c_2$	$s_1^2 s_2$
	$\sigma_{d(6)}$	\sim	$\overline{(1\ 3)(2)(4)}$	$a_1^2 c_2$	$s_1^2 s_2$
	$\sigma_{d(2)}$	\sim	$\overline{(1)(2)(3\ 4)}$	$a_1^2 c_2$	$s_1^2 s_2$
	$\sigma_{d(4)}$	\sim	$\overline{(1\ 2)(3)(4)}$	$a_1^2 c_2$	$s_1^2 s_2$
	$\sigma_{d(3)}$	\sim	$\overline{(1)(2\ 3)(4)}$	$a_1^2 c_2$	$s_1^2 s_2$
	$\sigma_{d(5)}$	\sim	$\overline{(1\ 4)(2)(3)}$	$a_1^2 c_2$	$s_1^2 s_2$
	$S_{4(3)}$	\sim	$\overline{(1\ 2\ 3\ 4)}$	c_4	s_4
	$S_{4(3)}^3$	\sim	$\overline{(1\ 4\ 3\ 2)}$	c_4	s_4
	$S_{4(1)}$	\sim	$\overline{(1\ 4\ 2\ 3)}$	c_4	s_4
	$S_{4(1)}^3$	\sim	$\overline{(1\ 3\ 2\ 4)}$	c_4	s_4
	$S_{4(2)}^3$	\sim	$\overline{(1\ 2\ 4\ 3)}$	c_4	s_4
	$S_{4(2)}$	\sim	$\overline{(1\ 3\ 4\ 2)}$	c_4	s_4

Table 4. Sphericities of Orbits [89].

G	G _i	Sphericity of G/(G _i)	Chirality fittingness (object allowed)	Sphericity index d	Dummy variable d
achiral	achiral	homospheric	achiral	a_d	S_d
achiral	chiral	enantiospheric	achiral, ^a chiral ^b	c_d	S_d
chiral	chiral	hemispheric	achiral, ^c chiral	b_d	S_d

^a An achiral object is restricted to be chiral. One half and the other half of the orbit are superimposable by a rotoreflection operator of G.

^b The orbit accommodates the half number ($|G|/2|G_i|$) of chiral objects and the half number of chiral objects of opposite chirality so as to accomplish compensated chiral packing

^c An achiral object is restricted to be chiral.

^d $d = |G|/|G_i|$ where $|G|$ and $|G_i|$ represent the respective orders.

The resulting orbits $\mathbf{C}_{3v}/(\mathbf{C}_s)$ and $\mathbf{C}_{3v}/(\mathbf{C}_{3v})$ are both homospheric, so that they are characterized by the sphericity indices a_3 and a_1 , because the sizes of these orbits are calculated to be $|\mathbf{C}_{3v}|/|\mathbf{C}_s| = 6/2 = 3$ and $|\mathbf{C}_{3v}|/|\mathbf{C}_{3v}| = 6/6 = 1$. Then, the total subduction (Eq. 7) is represented by the product a_1a_3 , which is called a *unit subduced cycle index with chirality fittingness* (USCICF). This term has been coined by keeping in mind the following scheme of derivation for combinatorial enumeration: *a unit subduced cycle index with chirality fittingness* (USCI-CF) \rightarrow *a subduced cycle index with chirality fittingness* (SCI-CF) \rightarrow *a cycle index with chirality fittingness* (CI-CF).

The procedure of subduction is repeated to cover all of the subgroups to give USCICFs as collected in the USCICF-column of Table 5. Note that \mathbf{T}_d has the following non-redundant set of subgroups (SSG):

$$\text{SSG}_{\mathbf{T}_d} = \{\mathbf{C}_1, \mathbf{C}_2, \mathbf{C}_s, \mathbf{C}_3, \mathbf{S}_4, \mathbf{D}_2, \mathbf{C}_{2v}, \mathbf{C}_{3v}, \mathbf{D}_{2d}, \mathbf{T}, \mathbf{T}_d\}, \quad (8)$$

where the subgroups are aligned in the ascending order of their orders after an appropriate representative is selected from each set of conjugate subgroups.

The data of subduction of $\mathbf{T}_d/(\mathbf{C}_{3v})$ collected in Table 5 can be applied in a qualitative fashion. The sphericity of each CR collected in the sphericity-column of Table 5 governs the mode of substitution according to the chirality fittingness shown in Figure 12. Thereby, a set of proligands is selected in accord with the chirality fittingness of each CR of a subgroup. For example, a \mathbf{C}_{3v} -molecule **39** shown in Figure 13 is generated by placing three achiral proligands A's on the homospheric $\mathbf{C}_{3v}/(\mathbf{C}_s)$ -orbit and one achiral proligand B on the homospheric $\mathbf{C}_{3v}/(\mathbf{C}_{3v})$ -orbit in accord with Eq. 7 (or the \mathbf{C}_{3v} -column of Table 5).

(a) Chirality fittingness of a homospheric orbit (sphericity index: a_d)

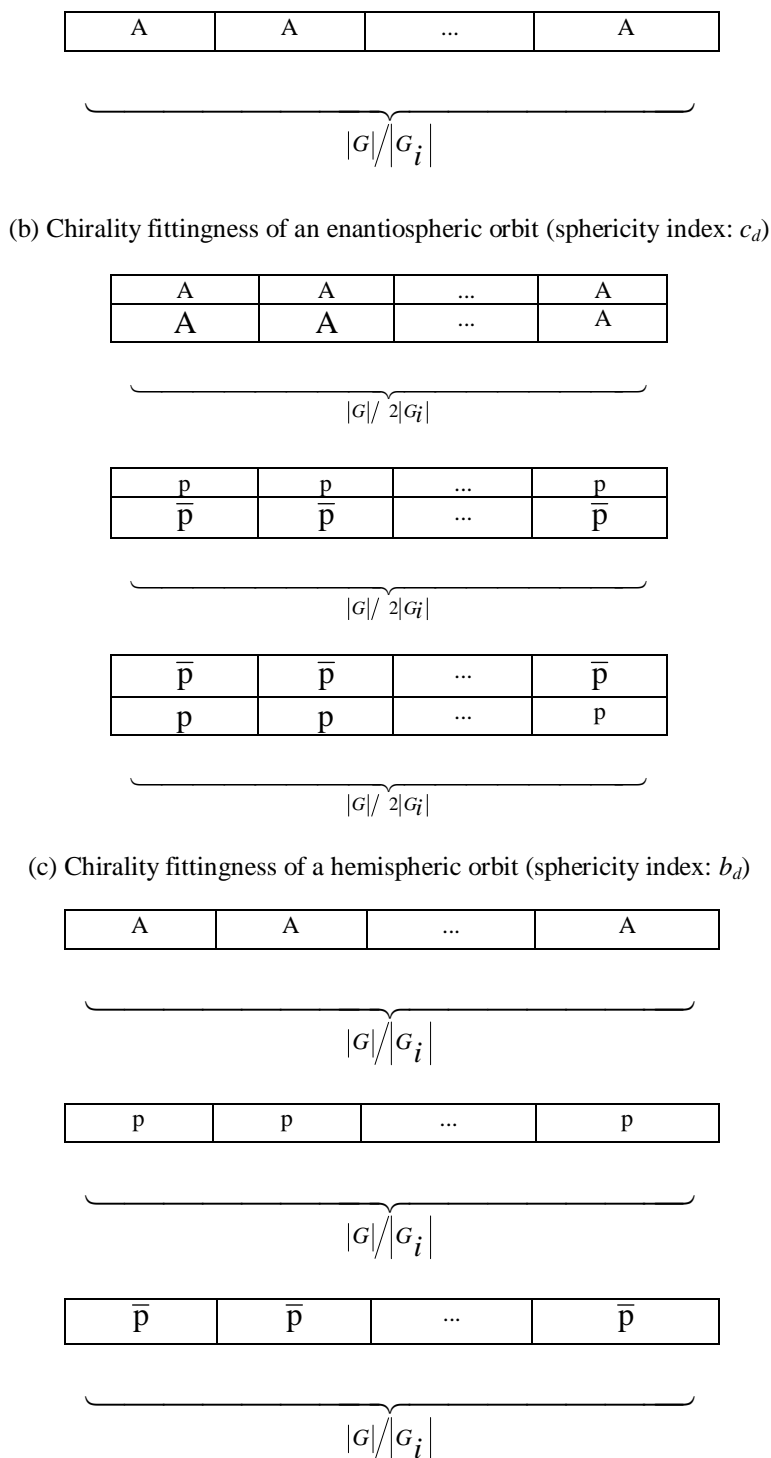


Figure 12. Chirality fittingness of orbits with three kinds of sphericities. The subscript d of each sphericity index is calculated to be $d = |G|/|G_i|$ [6, 89].

In a similar way, the data of the respective subductions collected in Table 5 can be used to generate the derivatives collected in Figure 13 by referring to the chirality

fittingness shown in Figure 12. A pair of derivatives linked with an underbrace is a pair of *RS*-diastereomers according to Fujita's stereoisogram approach [18].

From a qualitative point of view, Fujita's USCI approach enables us to rationalize various stereochemical phenomena in a systematic fashion [6, 7].

1. The first category of qualitative applications involves the methodology of molecular design: systematic derivation from methane and adamantane skeletons of *Td*-symmetry [94], systematic design of molecules of high symmetry [95], systematic design of chiral molecules of high symmetry [96], desymmetrization of achiral skeletons by monosubstitution [97], as well as chirality and stereogenicity for square-planar complexes [98].
2. The second category of qualitative applications is concerned with the proposal of the *SCR (subduction-of-coset-representation) notation*, which aims at systematic classification of molecular symmetries [91, 99].
3. The third category of qualitative applications is concerned with theoretical foundations, e.g., the proposal of the *proligand-promolecule model* and the formulation of *matched and mismatched molecules* [88], *chirogenic sites* in an enantiospheric orbit [100], characterization of prochirality and classification of meso-compounds [101], general treatments of local chirality and prochirality [89], as well as systematic characterization of prochirality, prostereogenicity, and stereogenicity by means of the sphericity concept [102].
4. The fourth category of qualitative applications is concerned with the merits of Fujita's USCI approach as compared with the conventional terminology of stereochemistry: stereochemistry and stereoisomerism characterized by the sphericity concept [93], an approach to topic relationships [103], approaches for restructuring stereochemistry by novel terminology [90, 104], and sphericity beyond topicity [86, 87]. Introductory discussions on importance of orbits and sphericity indices and on importance of local symmetries in subductions of coset representations have appeared in an internet journal [105, 106].

4.2.4. SYMMETRY-ITEMIZED ENUMERATION

Fujita's USCI approach supports four methods of symmetry-itemized enumeration of chemical compounds [6], i.e., the fixed-point-matrix (FPM) method [92, 107], the partial-cycle-index (PCI) method [108], the elementary-superposition (ES) method [109, 110], and the partial-superposition (PS) method [110].

The enumeration based on the tetrahedral skeleton **33** has been conducted by using the FPM method and the results have been reported in a tabular form (Table 1 of Ref. [88] and Table 21.1 of a book [6]). The PCI method is applied to the enumeration based on the tetrahedral skeleton **33** [93]. The results have been obtained in the form of generating

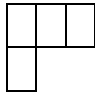
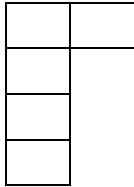
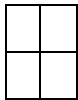

functions, where the coefficients of respective terms have been reported in a tabular form (Table 1 of Ref. [93]). Here, the PCI method applied to 33 [93] is described to show a representative embodiment of Fujita's USCI approach.

The USCI-CFs listed in Table 5 is aligned in accord with the SSG shown in Eq. 8:

$$\text{USCI-CF}_{T_d}(/C_{3v}) = (b_1^4, b_2^2, a_1^2 c_2, b_1 b_3, c_4, b_4, a_2^2, a_1 a_3, a_4, b_4, a_4), \quad (9)$$

Table 5. Subduction of a $T_d(/C_{3v})$ -Orbit [93].

Subgroup of T_d	Young 's tableau	Cycle structure	Subduction of $T_d(/C_{3v})$	Sphericity	USCI-CF					
T_d	<table><tr><td></td><td></td><td></td><td></td></tr></table>					4^1	$T_d(/C_{3v})$	homospheric a_4		
T	<table><tr><td></td><td></td><td></td><td></td></tr></table>					4^1	$T(/C_3)$	hemispheric b_4		
D_{2d}	<table><tr><td></td><td></td><td></td><td></td></tr></table>					4^1	$D_{2d}(/C_s)$	homospheric a_4		
C_{3v}	<table><tr><td></td><td></td><td></td></tr><tr><td></td><td></td><td></td></tr></table>							$3^1 1^1$	$C_{3v}(/C_s)$ $C_{3v}(/C_{3v})$	homospheric homospheric $a_1 a_3$
C_{2v}	<table><tr><td></td><td></td></tr><tr><td></td><td></td></tr></table>					2^2	$C_{2v}(/C_s)$ $C_{2v}(/C'_s)$	homospheric homospheric a_2^2		
D_2	<table><tr><td></td><td></td><td></td><td></td></tr></table>					4^1	$D_2(/C_1)$	hemispheric b_4		
S_4	<table><tr><td></td><td></td><td></td><td></td></tr></table>					4^1	$S_4(/C_1)$	enantiospheric c_4		

C_3		$3^1 1^1$	$C_3(/C_1)$ $C_3(/C_3)$	hemispheric hemispheric	$b_1 b_3$
C_s		$2^1 1^2$	$C_s(/C_1)$ $C_s(/C_s)$ $C_s(/C_s)$	enantiospheric homospheric homospheric	$a_1^2 c_2$
C_2		2^2	$C_2(/C_1)$ $C_2(/C_1)$	hemispheric hemispheric	b_2^2
C_1		1^4	$C_1(/C_1)$ $C_1(/C_1)$ $C_1(/C_1)$ $C_1(/C_1)$	hemispheric hemispheric hemispheric hemispheric	b_1^4

which is regarded as a formal row vector. Because of the subduction of a single CR, this formal row vector of USCI-CFs is considered to be a row vector of *subduced cycle indices with chirality fittingness* (SCI-CFs) according to Def. 19.3 of [6]. The formal vector (Eq. 9) is multiplied by the inverse mark table $M_{-1} T_d$ (Table B.10 shown in Appendix B of a book [6]) to give a formal vector:

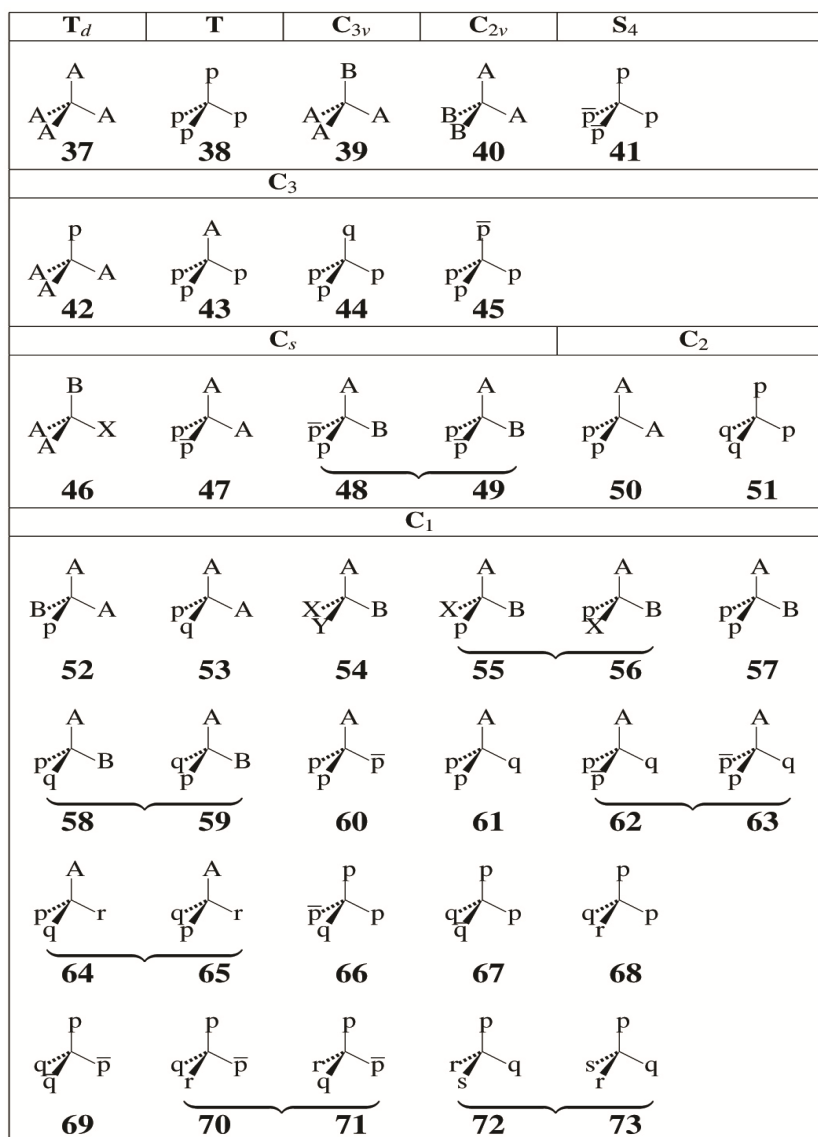


Figure 13. Promolecules from a tetrahedral skeleton [88].

$$(\dots, \text{PCI-CF}(\mathbf{G}_j), \dots) = \text{USCI-CF}_{T_d} (\mathcal{C}_{3v}) \times M_{T_d}^{-1}, \quad (10)$$

where the element $\text{PCI-CF}(\mathbf{G}_j)$ is the PCI-CF for each subgroup \mathbf{G}_j ($\mathbf{G}_j \in \text{SSG}_{T_d}$). See Def.19.6 of [6]. Thereby, PCI-CFs for every subgroups of SSG_{T_d} (Eq. 8) are obtained as follows:

$$\text{PCI-CF}(\mathbf{C}_1) = \frac{1}{24}b_1^4 - \frac{1}{8}b_2^2 - \frac{1}{4}a_1^2c_2 - \frac{1}{6}b_1b_3 + \frac{1}{4}b_4$$

$$+\frac{1}{4}a_2^2 + \frac{1}{2}a_1a_3 - \frac{1}{2}a_4 \quad (11)$$

$$\text{PCI-CF}(\mathbf{C}_2) = \frac{1}{4}b_2^2 - \frac{1}{4}c_4 - \frac{1}{4}b_4 - \frac{1}{4}a_2^2 + \frac{1}{2}a_4 \quad (12)$$

$$\text{PCI-CF}(\mathbf{C}_s) = \frac{1}{2}a_1^2c_2 - \frac{1}{2}a_2^2 - a_1a_3 + a_4; \quad (13)$$

$$\text{PCI-CF}(\mathbf{C}_3) = \frac{1}{2}b_1b_3 - \frac{1}{2}a_1a_3 - \frac{1}{2}b_4 + \frac{1}{2}a_4 \quad (14)$$

$$\text{PCI-CF}(\mathbf{S}_4) = \frac{1}{2}c_4 - \frac{1}{2}a_4 \quad (15)$$

$$\text{PCI-CF}(\mathbf{D}_2) = 0 \quad (16)$$

$$\text{PCI-CF}(\mathbf{C}_{2v}) = \frac{1}{2}a_2^2 - \frac{1}{2}a_4 \quad (17)$$

$$\text{PCI-CF}(\mathbf{C}_{3v}) = a_1a_3 - a_4 \quad (18)$$

$$\text{PCI-CF}(\mathbf{D}_{2d}) = 0 \quad (19)$$

$$\text{PCI-CF}(\mathbf{T}) = \frac{1}{2}b_4 - \frac{1}{2}a_4 \quad (20)$$

$$\text{PCI-CF}(\mathbf{T}_d) = a_4 \quad (21)$$

These PCI-CFs have been first noted in the articles by Fujita [86, 93].

Suppose that the four positions of **33** accommodate a set of proligands selected from the following proligand inventory:

$$\mathbf{L} = \{ \mathbf{A}, \mathbf{B}, \mathbf{X}, \mathbf{Y} ; \mathbf{p}, \bar{\mathbf{p}}, \mathbf{q}, \bar{\mathbf{q}}, \mathbf{r}, \bar{\mathbf{r}}, \mathbf{s}, \bar{\mathbf{s}} \}, \quad (22)$$

where the uppercase symbols, A, B, X, and Y, denote achiral proligands, while the paired lowercase symbols, p and $\bar{\mathbf{p}}$ etc., denote chiral proligands having opposite chirality senses. The chirality or achirality of each proligand is decided in isolation (when detached). Theorem 19.6 (or Theorem 9.7) of a book [6] permits us to adopt the following set of ligand-inventory functions:

$$a_d = \mathbf{A}^d + \mathbf{B}^d + \mathbf{X}^d + \mathbf{Y}^d \quad (23)$$

$$c_d = \mathbf{A}^d + \mathbf{B}^d + \mathbf{X}^d + \mathbf{Y}^d + 2\mathbf{p}^{d/2}\bar{\mathbf{p}}^{d/2} + 2\mathbf{q}^{d/2}\bar{\mathbf{q}}^{d/2} + 2\mathbf{r}^{d/2}\bar{\mathbf{r}}^{d/2} + 2\mathbf{s}^{d/2}\bar{\mathbf{s}}^{d/2} \quad (24)$$

$$b_d = \mathbf{A}^d + \mathbf{B}^d + \mathbf{X}^d + \mathbf{Y}^d + \mathbf{p}^d + \mathbf{q}^d + \mathbf{r}^d + \mathbf{s}^d + \bar{\mathbf{p}}^d + \bar{\mathbf{q}}^d + \bar{\mathbf{r}}^d + \bar{\mathbf{s}}^d. \quad (25)$$

It should be noted that the power $d/2$ appearing in Eq. 24 is an integer because the subscript d of c_d is always even in the light of the enantiosphericity of the corresponding orbit. See Table 4 and Figure 12 for the chirality fittingness of orbits.

The ligand-inventory functions (Eqs. 23–25) are introduced into the PCI-CFs (Eqs. 11–21). After expansion, we obtain the following generating functions [86, 93]:

$$\begin{aligned}
 f_{C_1} = & \{ (ABXp + ABX\bar{p}) + \dots \} + \{ (ABpq + AB\bar{p}q) \} + \dots \} \\
 & + \{ (Ap\bar{p}q + A\bar{p}p\bar{q}) + \dots \} + \{ (Apqr + A\bar{p}q\bar{r}) + \dots \} \\
 & + \{ (pqrs + \bar{p}q\bar{r}\bar{s}) + \dots \} + \{ (p\bar{p}qr + p\bar{p}q\bar{r}) + \dots \} \\
 & + \{ \frac{1}{2}(A^2Bp + A^2B\bar{p}) + \dots \} + \{ \frac{1}{2}(ABp^2 + AB\bar{p}^2) + \dots \} \\
 & + \{ \frac{1}{2}(A^2pq + A\bar{p}q) + \dots \} + \{ \frac{1}{2}(Ap^2\bar{p} + A\bar{p}p^2) + \dots \} \\
 & + \{ \frac{1}{2}(Ap^2q + A\bar{p}^2\bar{q}) + \dots \} + \{ \frac{1}{2}(p^2\bar{p}q + p\bar{p}^2\bar{q}) + \dots \} \\
 & + \{ \frac{1}{2}(p^2q\bar{q} + \bar{p}^2q\bar{q}) + \dots \} + \{ \frac{1}{2}(p^2qr + \bar{p}^2q\bar{r}) + \dots \} \\
 & + \{ p\bar{p}q\bar{q} + p\bar{p}r\bar{r} + \dots \} \\
 & + \{ ABXY \}
 \end{aligned} \tag{26}$$

$$f_{C_2} = \{ \frac{1}{2}(A^2p^2 + A^2\bar{p}^2) + \dots \} + \{ \frac{1}{2}(p^2q^2 + \bar{p}^2\bar{q}^2) + \dots \} \tag{27}$$

$$\begin{aligned}
 f_{C_s} = & \{ 2ABp\bar{p} + 2ABq\bar{q} + \dots \} + \{ A^2p\bar{p} + \dots \} \\
 & + \{ A^2BX + A^2BY + \dots \}
 \end{aligned} \tag{28}$$

$$\begin{aligned}
 f'_{C_3} = & \{ \frac{1}{2}(A^3p + A^3\bar{p}) + \dots \} + \{ \frac{1}{2}(Ap^3 + A\bar{p}^3) + \dots \} \\
 & + \{ \frac{1}{2}(p^3q + \bar{p}^3\bar{q}) + \dots \} + \{ \frac{1}{2}(p^3\bar{p} + p\bar{p}^3) + \dots \}
 \end{aligned} \tag{29}$$

$$f_{s_4} = \{ p^2\bar{p}^2 + q^2\bar{q}^2 + r^2\bar{r}^2 + s^2\bar{s}^2 \} \tag{30}$$

$$f_{C_{2v}} = \{ A^2B^2 + A^2X^2 + A^2Y^2 + \dots \} \tag{31}$$

$$f_{C_{3v}} = \{ A^3B + A^3X + A^3Y + \dots \} \tag{32}$$

$$f_T = \{ \frac{1}{2}(p^4 + \bar{p}^4) + \dots \} \tag{33}$$

$$f_{Td} = \{ A^4 + B^4 + X^4 + Y^4 \}. \tag{34}$$

In these generating functions, the coefficient of the term $A^a B^b X^x Y^y p^p \bar{p}^{\bar{p}} q^q \bar{q}^{\bar{q}} r^r \bar{r}^{\bar{r}} s^s \bar{s}^{\bar{s}}$ indicates the number of inequivalent (self-)enantiomeric pairs to be counted. Note that such a term as $1/2(ABXp + ABX\bar{p})$ indicates the presence of one enantiomeric pair of promolecules under the point-group symmetry. It follows that the term $(ABXp + ABX\bar{p})$ in the generating function f_{C_1} (Eq. 26) is interpreted to be $2 \times 1/2(ABXp + ABX\bar{p})$, which indicates the presence of two pairs of enantiomeric promolecules. The enumeration results represented by the generating functions (Eqs. 26–34) are consistent with the data listed in Tables 4 and 5 of Ref. [93] as tabular forms.

The promolecules enumerated by Eqs. 26–34 are depicted in Figure 13. Each pair of braces appearing in Eqs. 26–34 contains terms of the same pattern of substitution, e.g., A^4 , B^4 , X^4 , and Y^4 in f_{T_d} (Eq. 34), so that an appropriate representative (e.g., A^4) is depicted in Figure 13. Hence, 30 pairs of braces in Eqs. 26–34 corresponds to the 30 promolecules depicted in Figure 13, where a pair of promolecules linked with an underbrace (e.g., **48** and **49**) corresponds to the coefficient 2 of each term in a pair of braces (e.g., $2ABp\bar{p}$ in f_{C_s} of Eq. 28). Because a pair of (self-)enantiomers is counted once in Eqs. 26–34, an appropriate promolecule selected from a pair of enantiomers is depicted in Figure 13. A pair of promolecules linked with an underbrace in Figure 13 represents a pair of *RS*-diastereomers according to Fujita's stereoisogram approach, as will be discussed later.

The four methods supported by Fujita's USCI approach have been applied to symmetry-itemized enumerations starting from various skeletons, e.g., cage-shaped skeletons [111], adamantane isomers [112], non-rigid tetrahedral molecules [113], D_{3h} -skeletons [114], D_{2d} -skeletons [109], a dodecahedrane skeleton of I_h -symmetry [115], a fullerene skeleton of I_h -symmetry [108], imaginary transition structures for counting organic reactions [61], flexible six-membered skeletons [116], a benzene skeleton of D_{6h} -symmetry [117], ferrocene derivatives [118], a dumbbell skeleton of $D_{\infty h}$ -symmetry [119], an octahedral skeleton of O_h -symmetry [120, 121], and a cubane skeleton of O_h -symmetry [122, 123].

4.2.5. THE CONCEPT OF MANDALAS

The concept of *mandalas* has been proposed to give a diagrammatic introduction to Fujita's USCI approach in a series of articles [124, 125, 126]. Just as there appears an orbit of positions in a molecule (an intramolecular orbit), there appears an orbit of promolecules as an intermolecular orbit, which can be formulated by starting from the concept of mandalas. Group-theoretical foundations for the concept of mandalas have been discussed to bring about diagrammatic expressions for characterizing symmetries of 3D structures [127]. The

concept of mandalas has been applied to the diagrammatic formulation of Fujita's proligand method [128].

4.2.6. RESTRICTED ENUMERATIONS

The symmetry-itemized enumeration described above presumes that two or more orbits of vertices in a given skeleton accommodate proligands independently. In contrast, this presumption should be modified in symmetry-itemized enumeration of Kekulé structures, in which double bonds are not adjacent to each other. This type of restricted enumerations should take account of interaction between vertex substitution and edge substitution. For this purpose, the concept of *restricted subduced cycle indices* (RSCIs) has been proposed by Fujita [129].

The *restricted-subduced-cycle-index (RSCI) method* has been applied to symmetry-itemized enumeration of Kekulé structures of fullerene C₆₀ [129]. Fujita's RSCI method has been applied to counting matchings of graphs, so that it has been applied to Z-counting polynomials and the Hosoya index as well as to matching polynomials [130]. Fujita's RSCI method has been applied to enumeration of Kekulé structures in general and perfect matchings of graphs [131].

The FPM method of Fujita's USCI approach is modified to meet restricted conditions, so that the *restricted-fixed-point-matrix (RFPM) method* has been proposed on the basis of RSCIs [132]. The RFPM method has been applied to enumeration of three-dimensional structures derived from a dodecahedrane skeleton. The PCI method of Fujita's USCI approach is modified to meet restricted conditions, so that the *restricted-partial-cycle-index (RPCI) method* has been proposed on the basis of RSCIs [133]. The RPCI method has been applied to enumeration of three-dimensional structures derived from a dodecahedrane skeleton. A series of articles discussing general methods for treating interaction between two or more orbits has appeared [134, 135, 136].

4.3. FUJITA'S PROLIGAND METHOD AND RELATED METHODS

Although Fujita's USCI approach enables us to accomplish symmetry-itemized enumeration, gross enumeration without such symmetry-itemization is desirable if a brief perspective is necessary. The proligand method and related methods developed by Fujita are powerful to accomplish gross enumeration [9].

4.3.1. SPHERICITY OF CYCLES

Because each operation of a point group is a generator of a cyclic subgroup, the corresponding product of cycles can be correlated to the cyclic subgroup. Thereby, the concept of *sphericities of cycles* has been developed by Fujita [137], where it is correlated

to the concept of sphericities of orbits *for cyclic subgroups*. An odd- or even-cycle in a product of cycles for each operation of a point group is classified into three kinds as follows:

1. A d -cycle in a product of cycles for a (roto)reflection is classified to be a homospheric cycle, if d is odd. A sphericity index a_d is assigned to the homospheric d -cycle.
2. A d -cycle in a product of cycles for a (roto)reflection is classified to be an enantiospheric cycle, if d is even. A sphericity index c_d is assigned to the enantiospheric d -cycle.
3. A d -cycle in a product of cycles for a rotation is classified to be a hemispheric cycle, even if d is odd or even. A sphericity index b_d is assigned to the hemispheric d -cycle.

Then, the product of cycles for a (roto)reflection or a rotation is characterized by a *product of sphericity indices* (PSIs), which is calculated from the assigned sphericity indices for cycles. Table 3 collects such products of cycles for the respective operations of the CR $\mathbf{T}_d(\mathbf{C}_{3v})$, where the operations of subgroup \mathbf{T} represent rotations, while those of the coset $\mathbf{T}\sigma_{d(1)}$ represent (roto)reflections. For example, the rotation $\mathbf{C}_{3(1)}$ (a three-fold rotation) is denoted by the PSI b_1b_3 , because the 1-cycle (1) and the 3-cycle (2 3 4) are both hemispheric. On the other hand, the reflection $\sigma_{d(1)}$ (a dihedral reflection) is denoted by the PSI $a_1^2c_2$, because the 1-cycles (1) and (3) are homospheric as well as the 2-cycle (2 4) is enantiospheric.

It should be noted that the PSIs for cycles (cf. Table 3) are closely related to the USCI-CFs for orbits (cf. Table 5), where they are mediated through cyclic subgroups.

4.3.2. FUJITA'S PROLIGAND METHOD FOR GROSS ENUMERATION

Fujita's proligand method has been developed by using the PSIs defined above [137, 138, 139], so that we are able to accomplish gross enumeration of 3D structures under point groups.

According to Fujita's proligand method, a *cycle index with chirality fittingness* (CI-CF) is defined as the sum of PSIs for all of the operations of a given group, where the sum is divided by the order of the group [137]. For example, the PSIs listed in Table 3 are summed up and divided by the order of \mathbf{T}_d ($|\mathbf{T}_d| = 24$), so as to give the following CI-CF for the point group \mathbf{T}_d :

$$\text{CI} - \text{CF}(\mathbf{T}_d (/ \mathbf{C}_{3v})) = \frac{1}{24}(b_1^4 + 3b_2^2 + 8b_1b_3 + 6a_1^2c_2 + 6c_4). \quad (35)$$

Note that the CI-CF (Eq. 35) can be alternatively obtained by summing up the PCI-CFs (Eqs.11–21).

After ligand-inventory functions (e.g., Eqs. 23–25) for a ligand inventory (e.g., **L** represented by Eq. 22) are introduced into the CI-CF (e.g., Eq. 35), the resulting equation is expanded to give a generating function, in which the coefficient of each term represents the number of promolecules with the corresponding composition [137]. For example, the introduction of Eqs. 23–25 into Eq. 35 and the subsequent expansion provide a generating function for gross enumeration of promolecules on the basis of a tetrahedral skeleton **33**. Although the generating function is omitted here, it is equal to the sum of the symmetry-itemized generating functions represented by Eqs. 26–34.

4.3.3. FUJITA'S PROLIGAND METHOD VS. PÓLYA'S THEOREM

Pólya's theorem has been widely used to accomplish gross enumeration of chemical compounds as graphs [8, 60], where the action of permutation groups such as the symmetric group of degree 4 ($\mathbf{S}^{[4]}$) is presumed to control the behavior of graphs. As found by the terms 'graphs' and 'permutation groups', Pólya's theorem is incapable of enumerating *3D structures* (not 'graphs'), because it lacks the concept of *sphericities of cycles* under the action of *point groups* (not 'permutation groups') such as \mathbf{T}_d [140].

For example, Pólya's theorem uses a set of products of dummy variables collected in Table 3, which stems from the symmetric group of degree 4 ($\mathbf{S}^{[4]}$). Hence, the cycle index $\text{CI}(\mathbf{S}^{[4]})$ is calculated as follows:

$$\text{CI}(\mathbf{S}^{[4]}) = \frac{1}{24}(s_1^4 + 3s_2^2 + 8s_1s_3 + 6s_1^2s_2 + 6s_4). \quad (36)$$

The CI (Eq. 36) lacks sphericities of cycles in comparison with Eq. 35, which is obtained by using a set of products of sphericity indices (PSIs) on the basis of Fujita's proligand method. In other words, the three kinds of SIs (a_d , c_d , and b_d) in Eq. 35 (Fujita's proligand method) degenerate into one kind of dummy variables (s_d) in Eq. 36 (Pólya's theorem), so that 3D structures are projected into graphs.

A book concerning Fujita's proligand method and related enumeration tools has been published under the title "Combinatorial Enumeration of Graphs, Three-Dimensional Structures, and Chemical Compounds" [9]. The expression 'Graphs, Three-Dimensional Structures' in this title connotes a sharp contrast to the expression 'Graphs' in the title of Pólya's book "Combinatorial Enumeration of Groups, Graphs, and Chemical Compounds" [8].

4.3.4. RECURSIVE ENUMERATION OF MONOSUBSTITUTED ALKANES AND ALKANES

Fujita's prolignand method has been applied to the recursive enumeration of mono-substituted alkanes [141, 142] and alkanes [143, 144]. The results are shown in Table 6 [145], which also contains the results based on Pólya's theorem for the sake of comparison. Note that a pair of (self-)enantiomers is counted once by Fujita's prolignand method, while a constitution (graph) is counted once by Pólya's theorem.

Further recursive enumerations of monosubstituted alkanes and alkanes have been investigated by paying attention to various effects: structural effects [146], modes of categorization [145, 147], effects of asymmetric and pseudoasymmetric centers [148, 149], and effects of internal branching [150, 151]. Systematic comparison between 3D structures and graphs has been described [152, 153]. These results have been summarized to give a solution to a long-standing interdisciplinary problem over 130 years [154].

4.3.5. RELATED METHODS FOR GROSS ENUMERATION

The concept of sphericities of orbits in Fujita's USCI approach is closely related to the concept of sphericities of cycles in Fujita's prolignand method. The close relationship between these concepts can be demonstrated by several derivations of CI-CFs from USCI-CFs on the basis of the properties of inverse mark tables, which can be effectively restricted to cyclic subgroups. According to the procedures of such reduction, several methods of gross enumeration has been developed by Fujita [9], i.e., the markaracter method [155, 156], the characteristic-monomial (CM) method [157, 158, 159, 160, 161, 162], the extended-superposition (ExS) method [163], and the double-coset-representation (DCR) method [164]. Because these methods are based on the USCI approach, each of them requires a set of fundamental data (mark tables, inverse mark tables, subduction of coset representations, USCIs, and USCI-CFs), which are generally difficult to prepare in case of large groups. Hence, Fujita's prolignand method would be selected for the purpose of practical enumeration. It should be noted, however, that these related methods based on the USCI approach assure the Fujita's prolignand method and symmetry-itemized enumeration based on Fujita's USCI approach.

Table 6. Enumeration of Alkanes C_nH_{2n+2} [145].

n	Constitutional isomers by Pólya's theorem	3D structural isomers by Fujita's proligand method
1	1	1
2	1	1
3	1	1
4	2	2
5	3	3
6	5	5
7	9	9
8	18	19
9	35	38
10	75	88
11	159	203
12	355	509
13	802	1299
14	1858	3459
15	4347	9347
16	10359	25890
17	24894	72505
18	60523	205877
19	148284	589612
20	366319	1703575
21	910726	4954686
22	2278658	14502108
23	5731580	42671509
24	14490245	126180490
25	36797588	374749447
26	93839412	1117505952
27	240215803	3344714436
28	617105614	10045148539
29	1590507121	30264120901
30	4111846763	91449677878
31	10660307791	277096805630
32	27711253769	841783833517
33	72214088660	2563418291362
34	188626236139	7823943663908
35	493782952902	23931052067297

36	1295297588128	73345833181110
37	3404490780161	225226025743122
38	8964747474595	692862470624367
39	23647478933969	2135109239262173
40	62481801147341	6590223616010654
41	165351455535782	20372876580255143
42	438242894769226	63073132550694742
43	1163169707886427	195544793394384827
44	3091461011836856	607057684131345479
45	8227162372221203	1886989279103128211
46	21921834086683418	5872733742149957594
47	58481806621987010	18298681742426380229
48	156192366474590639	57080340544235225497
49	417612400765382272	178246302614039769705
50	1117743651746953270	557189473902522080578

By selecting cubane derivatives as probes of gross enumeration, Fujita's proliland method [165] has been compared with the markaracter method [166], the CM method [167], the ExS method [163], and the DCR method [164]. For the symmetry-itemized enumeration of cubane derivatives, see [122, 123].

4.4. FUJITA'S STEREOISOGRAM APPROACH

A given skeleton has been treated on the basis of a permutation group in the conventional methodology of stereochemistry, as Mislow and Siegel [168] pointed out that stereoisomers are recognized as prototypes of permutation isomers proposed by Ugi et al. [169]. On the other hand, a given skeleton has been treated on the basis of a point group in Fujita's USCI approach [6]. Even if the same skeleton is selected as a probe, the action of a permutation group is different from the action of a point group. For example, the action of the symmetric group of degree 4 ($S^{[4]}$) onto a tetrahedral skeleton **33** has been detailedly examined, so as to be different from the action of the point group T_d onto **33** [93]. Fujita's stereoisogram approach [10] has brought about Aufheben, in which point groups and permutation groups are integrated to create *RS*-stereoisomeric groups as a new category of groups.

4.4.1. DIFFERENCES BETWEEN POINT GROUPS AND PERMUTATION GROUPS

Figure 14 illustrates a set of stereoisomers of 2,3,4-trihydroxyglutaric acids (**74**, **74**, **75**, and **76**), which exhibits different behaviors towards the point group T_d and towards the symmetric group of degree 4 ($S^{[4]}$). Let us examine these stereoisomers according to Ref.

[93], after they are converted into the corresponding promolecules (**57**, $\overline{\mathbf{57}}$, **48**, and **49**) according to the proligand-promolecule model.

The symmetry-itemized enumeration under the action of the point group T_d [93] indicates the presence of one pair of enantiomers with the composition ABp_2 or ABp_2 (**57** and $\overline{\mathbf{57}}$, cf. the term $\frac{1}{2} (ABp^2 + AB\bar{p}^2)$ in f_{C_i} (Eq. 26)) and two achiral promolecules with the composition $ABp\bar{p}$ (**48** and **49**, cf. the term $2ABp\bar{p}$ in f_{C_s} (Eq. 28)). See Figure 14(a).

In contrast, the symmetry-itemized enumeration under the action of the permutation group $S^{[4]}$ [93] indicates the presence of one promolecule with the composition ABp^2 (**57**), one promolecule with the composition $AB\bar{p}^2$ ($\overline{\mathbf{57}}$), and one pair of **48** and **49**. See Figure 14(b). Because the conventional terminology of stereochemistry depends upon a pair of terms ‘chirality/achirality’ even under the action of $S^{[4]}$, the pairing of **48** (achiral) and **49** (achiral) cannot be rationalized, so that it is regarded as an exceptional case named ‘pseudoasymmetry’. Moreover, **57** with ABp^2 and $\overline{\mathbf{57}}$ with $AB\bar{p}^2$ are separately counted under $S^{[4]}$, where they are not recognized to give a pair of enantiomers.

In order to comprehend stereochemistry and stereoisomerism, I have proposed the stereoisogram approach [10], where the enumeration results of Figure 14(b) are harmonized with those of Figure 14(a). Thereby, **48** and **49** are recognized to be *RS*-stereogenic, so that they are pairwise counted once as a pair of *RS*-diastereomers under the action of an *RS*-permutation group which is isomorphic to the permutation group $S^{[4]}$. Moreover, **57** is *RS*-astereogenic and is not paired with $\overline{\mathbf{57}}$ (also *RS*-astereogenic) under the *RS*-permutation group.

4.4.2. RS-STEREISOMERIC GROUPS

According to Fujita’s stereoisogram approach [10, 11], a given point group can be extended to generate the corresponding *RS*-stereoisomeric group, which is characterized by a stereoisogram as a diagrammatic expression. As a typical example, let us examine the point group T_d (order 24), which can be extended to generate the corresponding *RS*-stereoisomeric group $T_{d\bar{\sigma}1}$ (order 48).

The point group T_d for the tetrahedral skeleton **33** is decomposed as follows:

$$T_d = T + T\sigma, \quad (37)$$

where the symbol σ is a representative selected from the 12 (roto)reflection operations of T_d (the $T_{\sigma d(1)}$ part of Table 3). The coset decomposition shown by Eq. 37 characterizes an enantiomeric relationship between **33** (and its homomers; A) and **33** (and its homomers; B), as shown in the vertical direction of Figure 15.

An *RS-permutation* denoted by the symbol $\tilde{\sigma}$ is defined as an operation which has the same permutation as σ but no alternation of chirality. Then, the *RS-permutation group* $\mathbf{T}_{\tilde{\sigma}}$ is defined as follows:

$$\mathbf{T}_{\tilde{\sigma}} = \mathbf{T} + \mathbf{T}\tilde{\sigma}, \quad (38)$$

which has been noted previously (Eq. 44 of [170]). The *RS-permutation group* $\mathbf{T}_{\tilde{\sigma}}$ is isomorphic to the symmetric group of degree 4 ($\mathbf{S}^{[4]}$), so that $\mathbf{T}_{\tilde{\sigma}}$ and $\mathbf{S}^{[4]}$ can be equalized for practical purposes of enumerating tetrahedral promolecules. The coset decomposition shown by Eq. 38 characterizes an *RS-diastereomeric relationship* between **33** (and its homomers; A) and **77** (and its homomers; C), as shown in the horizontal direction of Figure 15.

A ligand reflection is defined as an operation which has the same permutation as a rotation ($\in \mathbf{T}$) but alternation of chirality. Let the symbol \hat{I} represent an operation which has the same permutation as I but alternation of chirality. Thereby, the *ligand-reflection group* $\mathbf{T}_{\hat{I}}$ is defined as follows:

$$\mathbf{T}_{\hat{I}} = \mathbf{T} + \mathbf{T}\hat{I}, \quad (39)$$

which has been noted previously (Eq. 57 of [170]). Then, there appear 12 ligand reflections contained the coset $\mathbf{T}\hat{I}$. The coset decomposition shown by Eq. 39 characterizes a *holantimeric relationship* between **33** (and its homomers; A) and **77** (and its homomers; D), as shown in the diagonal direction of Figure 15.

Because the group \mathbf{T} contained in Eqs. 37–39 as a common subgroup, the *RS-stereoisomeric group* $\mathbf{T}_{d\tilde{\sigma}\hat{I}}$ can be formulated as follows:

$$\mathbf{T}_{d\tilde{\sigma}\hat{I}} = \mathbf{T} + \mathbf{T}\sigma + \mathbf{T}\tilde{\sigma} + \mathbf{T}\hat{I}, \quad (40)$$

where the group \mathbf{T} is a normal subgroup of $\mathbf{T}_{d\tilde{\sigma}\hat{I}}$. This coset decomposition has been noted previously (Eq. 8 of [170]).

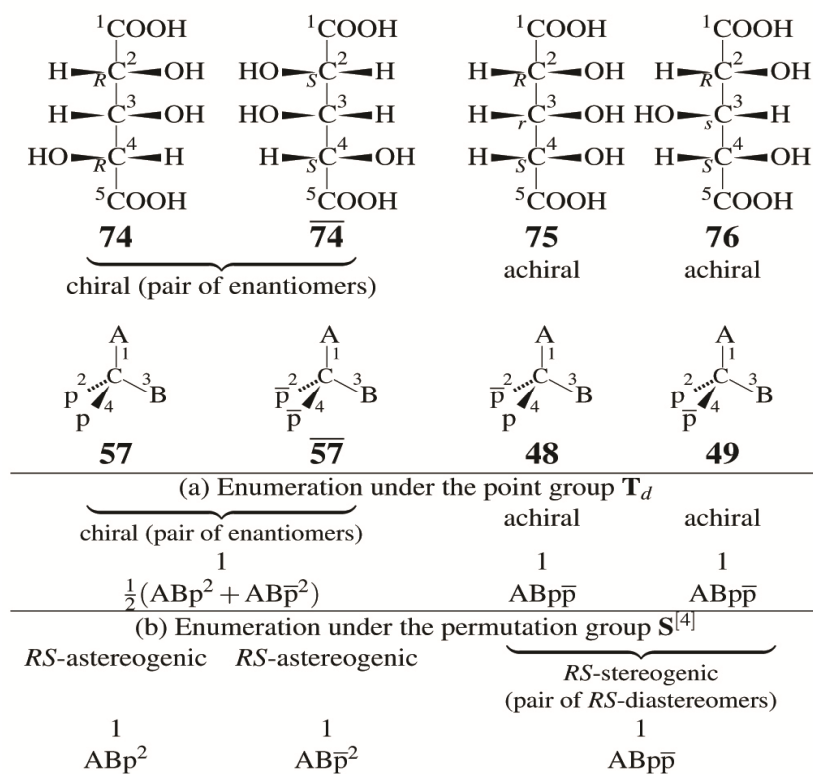


Figure 14. 2,3,4-Trihydroxyglutaric acids and the corresponding promolecules: (a) the itemized numbers under the point group T_d and (b) the itemized numbers under the permutation group $\text{S}^{[4]}$. The two achiral derivatives (**75** and **76**) or the corresponding promolecules (**48** and **49**) exhibit a pseudoasymmetric feature.

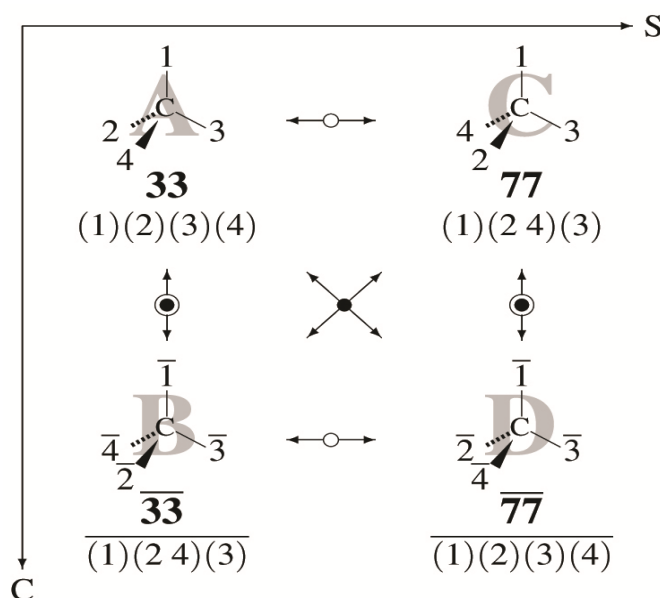


Figure 15. Elementary stereoisogram of numbered tetrahedral skeletons. The other modes of sequential numbering are permitted without losing generality [13].

The respective cosets of Eq. 40 correspond to the skeletons depicted in Figure 15, i.e., \mathbf{T} to 33 (and its homomers; A), $\mathbf{T}\sigma$ to $\overline{33}$ (and its homomers; B), $\mathbf{T}\tilde{\sigma}$ to 77 (and its homomers; C), and $\mathbf{T}\hat{\sigma}$ to $\overline{77}$ (and its homomers; D). These skeletons are referred to as being *RS*-stereoisomeric to one another under the action of the *RS*-stereoisomeric group $\mathbf{T}_{d\hat{\sigma}\hat{\tau}}$ (Eq. 40). The resulting diagram (Figure 15) is called an *elementary stereoisogram* of numbered tetrahedral skeletons [13]. Thus, a quadruplet of numbered tetrahedral skeletons is controlled by the *RS*-stereoisomeric group $\mathbf{T}_{d\hat{\sigma}\hat{\tau}}$ (Eq. 40).

4.4.3. FIVE TYPES OF STEREOISOGRAMS

Because the subgroup \mathbf{T} is a normal subgroup of the *RS*-stereoisomeric group $\mathbf{T}_{d\hat{\sigma}\hat{\tau}}$, the coset decomposition represented by Eq. 40 provides the following factor group [171]:

$$\mathbf{T}_{d\hat{\sigma}\hat{\tau}}/\mathbf{T} = \{\mathbf{T}, \mathbf{T}\sigma, \mathbf{T}\tilde{\sigma}, \mathbf{T}\hat{\sigma}\}, \quad (41)$$

which is isomorphic to Klein's four-group or the point group \mathbf{C}_{2v} . Because the numbered tetrahedral skeletons of the elementary stereoisogram (Figure 15) correspond to the respective cosets appearing in Eq. 41, a quadruplet of the numbered tetrahedral skeletons is found to be controlled by the factor group $\mathbf{T}_{d\hat{\sigma}\hat{\tau}}/\mathbf{T}$ (Eq. 41).

Just as Klein's four-group has five subgroups, the factor group $\mathbf{T}_{d\hat{\sigma}\hat{\tau}}/\mathbf{T}$ (Eq. 41) has the following five subgroups:

$$\text{Type I: } \mathbf{T}_i/\mathbf{T} \text{ (cf. Eq. 39)} \quad (42)$$

$$\text{Type II: } \mathbf{T}_{\bar{\sigma}}/\mathbf{T} \text{ (cf. Eq. 38)} \quad (43)$$

$$\text{Type III: } \mathbf{T}/\mathbf{T} \quad (44)$$

$$\text{Type IV: } \mathbf{T}_{d\bar{\sigma}\bar{i}}/\mathbf{T} \text{ (cf. Eq. 40)} \quad (45)$$

$$\text{Type V: } \mathbf{T}_d/\mathbf{T} \text{ (cf. Eq. 37),} \quad (46)$$

which correspond to $\mathbf{T}_{d\bar{\sigma}\bar{i}}/\mathbf{T}$ (Eq. 40) itself and its maximum subgroups (Eqs. 37–39) as well as the common normal subgroup \mathbf{T} .

By placing a set of proligands to the four-positions of each tetrahedral skeleton of the elementary stereoisogram (Figure 15), there appear a *stereoisogram* containing a quadruplet of promolecules, where an equality symbol is placed in vertical, horizontal, or diagonal directions if two promolecules in each direction are identical with each other. Meanwhile, the global symmetry $\mathbf{T}_{d\bar{\sigma}\bar{i}}/\mathbf{T}$ (Eq. 41) is restricted to one of the five subgroups (Eqs. 42–46), which is assigned to the generated stereoisogram.

A set of proligands ABp^2 is placed on the four positions of the skeleton **33** (Figure 15), so as to generate the promolecule **57** (Figure 14) as a reference promolecule. Thereby, there appears a stereoisogram shown in Figure 16. The stereoisogram belongs to type II, which is characterized by the presence of horizontal equality symbols. Such a type-II stereoisogram is determined to be chiral, *RS*-astereogenic, and scleral, so as to be denoted by the type index $[-, a, -]$. It should be noted that the quadruplet of promolecules (**57**, $\overline{\mathbf{57}}$, $\mathbf{57}'$ ($= \mathbf{57}$), and $\overline{\mathbf{57}}'$ ($= \overline{\mathbf{57}}$)) is regarded as one equivalence class of *RS*-stereoisomers, which is interpreted to be a pair of enantiomers (**57** and $\overline{\mathbf{57}}$).

By placing a set of proligands $\text{ABp}\bar{\text{p}}$ on the four positions of the skeleton **33** (Figure 15), the promolecule **48** (Figure 17) is generated as a reference promolecule. Thereby, there appears a stereoisogram shown in Figure 17. The stereoisogram belongs to type V, which is characterized by the presence of vertical equality symbols. Such a type-V stereoisogram is determined to be achiral, *RS*-stereogenic, and scleral, so as to be denoted by the type index $[a, -, -]$. It should be noted that the quadruplet of promolecules (**48**, $\overline{\mathbf{48}}$ ($= \mathbf{48}$), **49**, and $\overline{\mathbf{49}}$ ($= \mathbf{49}$)) is regarded as one equivalence class of *RS*-stereoisomers, which is interpreted to be one pair of *RS*-diastereomers **48** and **49**. The achirality of **48** or **49** is assured by the vertical equality symbol, which indicates that **48** (or **49**) is self-enantiomeric.

A set of proligands ABXY is placed on the four positions of the skeleton **33** (Figure 15) so as to generate the promolecule **54** (Figure 18) as a reference promolecule. Thereby, there appears a stereoisogram shown in Figure 18. The stereoisogram belongs to type I, which is characterized by the presence of diagonal equality symbols. Such a type-I stereoisogram is determined to be chiral, *RS*-stereogenic, and ascleral, so as to be denoted by the type index $[-, -, a]$. It should be noted that the quadruplet of promolecules (**54**, $\overline{\mathbf{54}}$,

$\mathbf{54}' (= \mathbf{54})$, and $\overline{\mathbf{54}}' (= \mathbf{54})$) is regarded as one equivalence class of *RS*-stereoisomers, which is interpreted to be one pair of enantiomers $\mathbf{54}$ and $\overline{\mathbf{54}}$

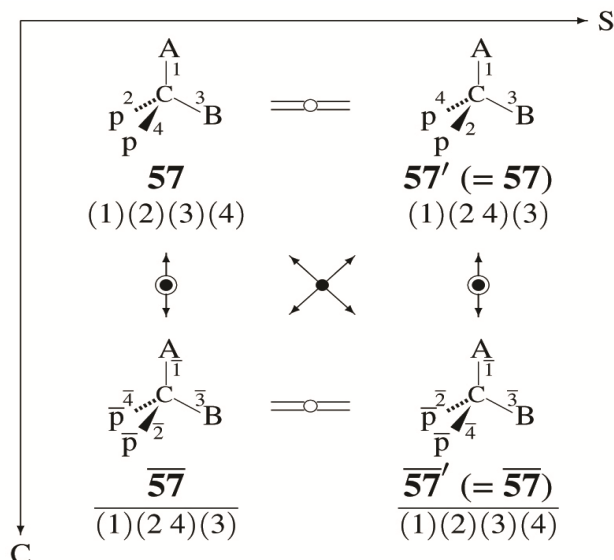


Figure 16. Stereoisogram of type II for characterizing a quadruplet of *RS*-stereoisomers with the composition ABp^2 or $AB\bar{p}^2$ on the basis of a tetrahedral skeleton. This stereoisogram contains one pair of enantiomers [172].

In addition, there appear type-III and type-IV stereoisograms as two extreme types of stereoisograms. A type-III stereoisogram characterized by the absence of equality symbols in all the directions, while a type-IV stereoisogram characterized by the presence of equality symbols in all the directions.

Figure 19 collects stereoisograms of five types, each of which represents a quadruplet of

RS-stereoisomers, where the symbols A and A (or B and B) represent a pair of enantiomeric promolecules [12]. A type-III stereoisogram exhibits an extreme feature, in which the four *RS*-stereoisomers (i.e., \mathbf{A} , $\overline{\mathbf{A}}$, \mathbf{B} and $\overline{\mathbf{B}}$) are different from one another. A type-IV stereoisogram exhibits another extreme feature, in which the appears a degenerate *RS*-stereoisomer (i.e., \mathbf{A})[10, 12].

The merits of stereoisograms have been discussed from a viewpoint of a new scheme for investigating geometric and stereoisomeric features [173]. Fujita's stereoisogram approach has been applied to allene derivatives [174], trigonal bipyramidal compounds [175, 176], prismane derivatives [177, 178], octahedral complexes [179, 180], and cubane derivatives [181].

To discuss local symmetries, the concept of *correlation diagrams of stereoisograms* has been proposed by Fujita [182, 183, 184]. Theory of organic stereoisomerism in harmony with molecular symmetry has been demonstrated [185].

It is worthwhile to mention discrimination between *RS*-stereoisomeric groups and stereoisomeric groups in assigning *E/Z*-descriptors to ethylene derivatives [186]. Such stereoisomeric groups are concerned with *extended stereoisogram sets* for characterizing *E/Z*-descriptors and *cis,trans*-isomerizations, the latter of which have been represented by a *radical space* in Fujita's ITS approach [58].

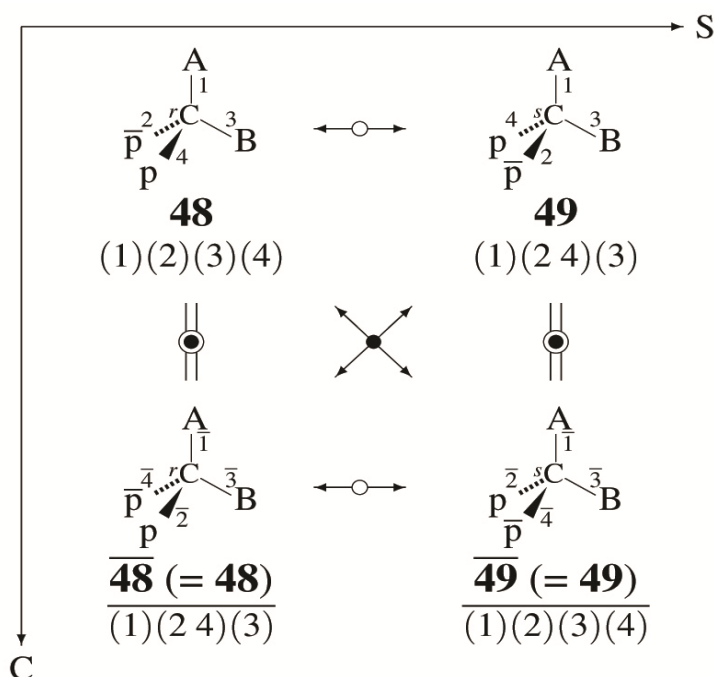


Figure 17. Stereoisogram of type V for characterizing a quadruplet of *RS*-stereoisomers with the composition $ABp\bar{p}$ on the basis of a tetrahedral skeleton. This stereoisogram contains two achiral promolecules [172].

4.4.4. NEW THEORETICAL FOUNDATIONS FOR R/S-DESCRIPTORS

A pair of *R/S*-descriptors of the Cahn-Ingold-Prelog (CIP) system [16, 17] has been used to specify a pair of enantiomers (e.g., a pair of **54** and **54**; an asymmetric case) and a pair of diastereomers (**48** and **49**; a pseudoasymmetric case). The term 'chirality' has been originally used to rationalize the CIP system [16], so that the pairing of diastereomers (e.g., **48** and **49**) has not been supported by a sufficient theoretical foundation. The term 'stereogenicity' in place of the term 'chirality' has been later used to rationalize these conflicting cases [17] after the discussions by Mislow and Siegel [168]. However, the term

‘stereogenicity’ also covers *Z/E*-descriptors for specifying a diastereomeric relationship [187]. This usage of ‘stereogenicity’ in modern stereochemistry is misleading because chirality and stereogenicity are not clearly differentiated from each other. In particular, a pair of chirality/achirality is solely taken into consideration, so that the interaction between chirality and stereogenicity is underestimated or disregarded in modern stereochemistry.

According to Fujita’s stereoisogram approach [10, 11, 12], in contrast, there appear three pairs of attributes (or three pairwise relationships): that is to say, a pair of chirality/achirality (enantiomeric and self-enantiomeric relationships in the vertical directions of a stereoisogram), a pair of *RS*-stereogenicity/*RS*-astereogenicity (*RS*-diastereomeric or self-*RS*-diastereomeric relationships in the horizontal direction), and a pair of sclerality/asclerality (holantimeric or selfholantimeric relationships in the diagonal direction).

An important conclusion of Fujita’s stereoisogram approach is that a pair of *R/S*-descriptors is originally assigned to a pair of *RS*-diastereomers, not to a pair of enantiomers, where an *RS*-diastereomeric relationship stems from *RS*-stereogenicity inherent in a stereoisogram of type I, type III, or type V (see Figure 19) [13, 188]. Three aspects of absolute configuration (the chiral aspect, the *RS*-stereogenic aspect, and the scleral aspect) have been pointed out on the basis of Fujita’s stereoisogram approach, so as to revise the conventional terminology based on a single chiral aspect of absolute configuration [189].

For example, a pair of *RS*-diastereomers **48** and **49** in the type-V stereoisogram (Figure 17) is specified by a pair of lowercase labels ‘*r*’ and ‘*s*’, where the priority sequence $A > B > p > \bar{p}$ is presumed. This example clearly demonstrates that a pair of *R/S*-descriptors is assigned on the basis of the *RS*-stereogenic aspect, not on the basis of the chiral aspect of absolute configuration, because both **48** and **49** are achiral. Hence, the lowercase labels stems from the chirality-unfaithful nature [190].

Along the same line, a pair of *RS*-diastereomers **54** and **54'** ($= \overline{\mathbf{54}}$) in the type-I stereoisogram (Figure 18) is specified by a pair of uppercase labels ‘*R*’ and ‘*S*’, where the priority sequence $A > B > X > Y$ is presumed. Because the *RS*-diastereomeric relationship is coincident with the enantiomeric relationship in such a type-I stereoisogram, the pair of labels ‘*R*’ and ‘*S*’, which is originally assigned to the pair of *RS*-diastereomers **54** and **54'** (due to the *RS*-stereogenic aspect), is interpreted to be assigned to the pair of enantiomers **54** and $\overline{\mathbf{54}}$ (due to the chiral aspect). Note that the uppercase labels stems from the chirality-faithful nature [190].

Misleading standpoints for *R/S*-descriptors of the CIP system have been rationally avoided by Fujita’s stereoisogram approach [14, 191]. Moreover, misleading classification of isomers and stereoisomers in organic chemistry has been discussed by emphasizing equivalence relationships and equivalence classes [192]. A recent book by Fujita [18] deals with the feasibility of Fujita’s stereoisogram approach in detail.

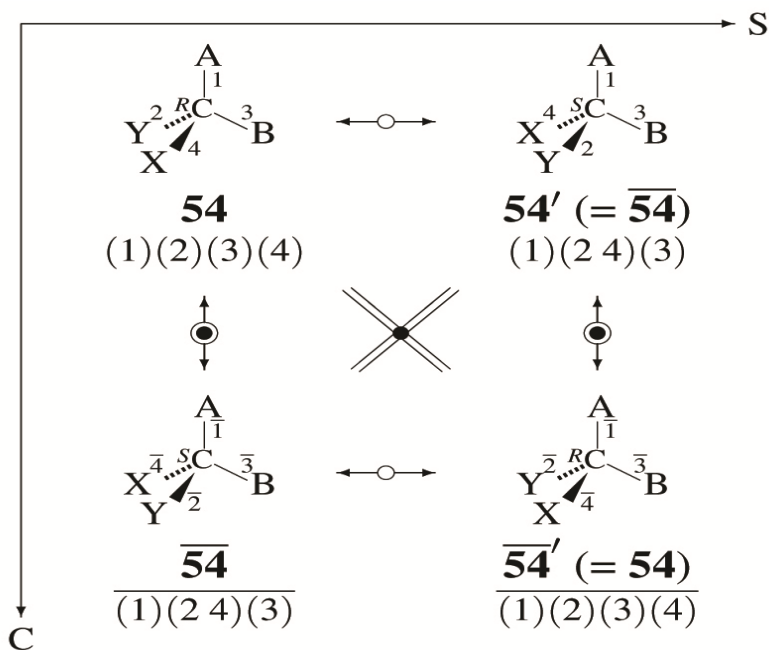


Figure 18. Stereoisogram of type I for characterizing a quadruplet of *RS*-stereoisomers with the composition ABXY on the basis of a tetrahedral skeleton. This stereoisogram contains one pair of enantiomers [172].

4.4.5. PROCHIRALITY VS. PRO-*RS*-STEREOGENICITY

The formulation of Fujita's USCI approach teaches us that the term *prochirality* should be used in a purely geometrical fashion [89]. According to Fujita's stereoisogram approach, the concept of *pro-*RS*-stereogenicity* [193, 194] has been proposed to settle long-standing confusion on the term 'prochirality' of Hanson's definition [195].

As pointed out in recent articles [15, 196, 191], Hanson's definition of the term 'prochirality' for giving *pro-R/pro-S*-descriptors [195] should be abandoned. A pair of *pro-R/pro-S*-descriptors should be assigned on the basis of *pro-*RS*-stereogenicity* (not Hanson's 'prochirality'), just as a pair of *R/S*-descriptors should be assigned on the basis of *RS*-stereogenicity (not 'chirality' nor 'stereogenicity') [13, 14, 197].

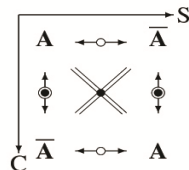
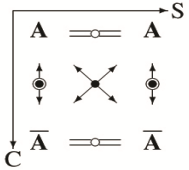
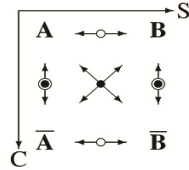
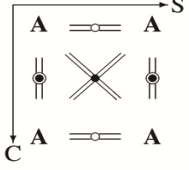
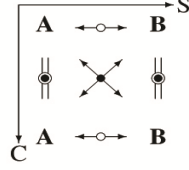
	<i>RS</i> -astereogenic	<i>RS</i> -stereogenic
chiral		Type I: $[-, -, a]$ chiral/ <i>RS</i> -stereogenic/ascleral  two promolecules one pair of enantiomers one pair of <i>RS</i> -diastereomers two ascleral promolecules one quadruplet of <i>RS</i> -stereoisomers
	Type II: $[-, a, -]$ chiral/ <i>RS</i> -astereogenic/scleral  two promolecules one pair of enantiomers two <i>RS</i> -astereogenic promolecules one pair of holantimers one quadruplet of <i>RS</i> -stereoisomers	Type III: $[-, -, -]$ chiral/ <i>RS</i> -stereogenic/scleral  four promolecules two pairs of enantiomers two pairs of <i>RS</i> -diastereomers two pairs of holantimers one quadruplet of <i>RS</i> -stereoisomers
achiral	Type IV: $[a, a, a]$ achiral/ <i>RS</i> -astereogenic/ascleral  one promolecule one achiral promolecule one <i>RS</i> -astereogenic promolecule one ascleral promolecule one quadruplet of <i>RS</i> -stereoisomers	Type V: $[a, -, -]$ achiral/ <i>RS</i> -stereogenic/scleral  two promolecules two achiral promolecules one pair of <i>RS</i> -diastereomers one pair of holantimers one quadruplet of <i>RS</i> -stereoisomers

Figure 19. Stereoisograms for representing *RS*-stereoisomers of five types [12]. The symbols **A** and $\overline{\mathbf{A}}$ (or **B** and $\overline{\mathbf{B}}$) represent a pair of enantiomers. Each stereoisogram consists of a quadruplet of *RS*-stereoisomers, which may coalesce with one another according to either one of the five *RS*-stereoisomeric types.

Substitution criteria based on stereoisograms have been proposed to determine prochirality and pro-*RS*-Stereogenicity [198]. The term *RS-diastereotopic relationship* has been coined to specify *pro-R/pro-S*-descriptors [199]. The term ‘stereoheterotopic relationship’ [200] should be abandoned because it connotes ‘enantiotopic’ (due to chirality) and ‘diastereotopic’ (due to stereogenicity) which are conceptually different.

The merits of Fujita’s stereoisogram approach in discussions on prochirality vs. pro-*RS*-stereogenicity have been demonstrated by recent articles [15, 201, 202].

4.4.6. ENUMERATION OF INEQUIVALENT QUADRUPLTS OF *RS*-STEREISOMERS

The FPM method and the PCI method supported by Fujita’s USCI approach have been extended to meet the requirements of Fujita’s stereoisogram approach [203, 204].

The symmetry-itemized enumeration of quadruplets of *RS*-stereoisomers based on a tetrahedral skeleton **33** has been conducted by an extended FPM method [203] or by an extended PCI method [204] under the action of the *RS*-stereoisomeric group $\mathbf{T}_{d\tilde{\sigma}\hat{i}}$. This *RS*-stereoisomeric group has 33 subgroups up to conjugacy to provide a non-redundant set of subgroups (SSG):

$$\begin{aligned} \text{SSG}_{\mathbf{T}_{d\tilde{\sigma}\hat{i}}} = & \left\{ \overset{1}{\mathbf{C}_1}, \overset{2}{\mathbf{C}_2}, \overset{3}{\mathbf{C}_{\hat{\sigma}}}, \overset{4}{\mathbf{C}_{\tilde{\sigma}}}, \overset{5}{\mathbf{C}_s}, \overset{6}{\mathbf{C}_{\hat{i}}}, \overset{7}{\mathbf{C}_3}, \overset{8}{\mathbf{S}_{\tilde{4}}}, \overset{9}{\mathbf{S}_4}, \overset{10}{\mathbf{D}_2}, \right. \\ & \overset{11}{\mathbf{C}_{2\tilde{\sigma}}}, \overset{12}{\mathbf{C}_{2\hat{\sigma}}}, \overset{13}{\mathbf{C}_{2v}}, \overset{14}{\mathbf{C}_s\tilde{\sigma}\hat{\sigma}}, \overset{15}{\mathbf{C}_{2\hat{i}}}, \overset{16}{\mathbf{C}_s\tilde{\sigma}\hat{\sigma}}, \overset{17}{\mathbf{C}_3\tilde{\sigma}}, \overset{18}{\mathbf{C}_{3v}}, \\ & \overset{19}{\mathbf{C}_3\hat{i}}, \overset{20}{\mathbf{D}_{2\tilde{\sigma}}}, \overset{21}{\mathbf{S}_{\tilde{4}\hat{\sigma}}}, \overset{22}{\mathbf{S}_{\tilde{4}\hat{i}}}, \overset{23}{\mathbf{D}_{2d}}, \overset{24}{\mathbf{S}_{4\tilde{\sigma}\hat{\sigma}}}, \overset{25}{\mathbf{D}_{2\hat{i}}}, \overset{26}{\mathbf{C}_{2v}\tilde{\sigma}\hat{i}}, \\ & \left. \overset{27}{\mathbf{T}}, \overset{28}{\mathbf{C}_{3d}\tilde{\sigma}\hat{i}}, \overset{29}{\mathbf{C}_{3v}\tilde{\sigma}\hat{i}}, \overset{30}{\mathbf{D}_{2d}\tilde{\sigma}\hat{i}}, \overset{31}{\mathbf{T}_{\tilde{\sigma}}}, \overset{32}{\mathbf{T}_{\hat{i}}}, \overset{33}{\mathbf{T}_d}, \mathbf{T}_{d\tilde{\sigma}\hat{i}} \right\} \end{aligned} \quad (47)$$

where the subgroups are aligned in the ascending order of their orders.

The four positions of **33** belongs to an orbit governed by the coset representation the $\mathbf{T}_{d\tilde{\sigma}\hat{i}}(/ \mathbf{C}_{3v\tilde{\sigma}\hat{i}})$, degree of which is calculated to be $|\mathbf{T}_{d\tilde{\sigma}\hat{i}}|(| \mathbf{C}_{3v\tilde{\sigma}\hat{i}} |) = 48/12 = 4$. The subduction of $\mathbf{T}_{d\tilde{\sigma}\hat{i}}(/ \mathbf{C}_{3v\tilde{\sigma}\hat{i}})$, can be conducted in an extended fashion, so as to generate USCI-CFs under the *RS*-stereoisomeric group $\mathbf{T}_{d\tilde{\sigma}\hat{i}}$

The fixed-point matrix (FPM) method of the USCI approach is applied to the extended USCI-CFs. Thereby, the numbers of quadruplets are calculated in an itemized fashion with respect to the subgroups of $\mathbf{T}_{d\tilde{\sigma}\hat{i}}$, where they are given in a matrix (tabular) form [203]. In a parallel way, the PCI method of the USCI approach is applied to the extended USCI-CFs. Thereby, the numbers of quadruplets are calculated in an itemized

fashion with respect to the subgroups of $\mathbf{T}_{d\bar{\sigma}\hat{i}}$, where they are given in the form of generating functions [204]. Several generating functions are cited as follows (Eqs. 44–48 of Ref. [204]):

$$f_{c_1} \stackrel{\text{I}}{=} \left\{ \frac{1}{2} (\text{ABXp} + \text{ABX}\bar{\text{p}}) + \cdots \right\} + \left\{ \frac{1}{2} (\text{ABpq} + \text{AB}\bar{\text{p}}\bar{\text{q}}) + \cdots \right\} \\ + \left\{ \frac{1}{2} (\text{Ap}\bar{\text{p}}\text{q} + \text{A}\bar{\text{p}}\text{p}\bar{\text{q}}) + \cdots \right\} + \left\{ \frac{1}{2} (\text{Apqr} + \text{A}\bar{\text{p}}\bar{\text{q}}\bar{\text{r}}) + \cdots \right\} \\ + \left\{ \frac{1}{2} (\text{pqrs} + \bar{\text{p}}\bar{\text{q}}\bar{\text{r}}\bar{\text{s}}) + \cdots \right\} + \left\{ \frac{1}{2} (\text{p}\bar{\text{p}}\text{qr} + \bar{\text{p}}\bar{\text{p}}\bar{\text{q}}\bar{\text{r}}) + \cdots \right\} \quad (48)$$

$$f_{c_{\bar{\sigma}}} \stackrel{\text{II}}{=} \left\{ \frac{1}{2} (\text{A}^2\text{Bp} + \text{A}^2\text{B}\bar{\text{p}}) + \cdots \right\} + \left\{ \frac{1}{2} (\text{ABp}^2 + \text{AB}\bar{\text{p}}^2) + \cdots \right\} \\ + \left\{ \frac{1}{2} (\text{A}^2\text{pq} + \text{A}^2\bar{\text{p}}\bar{\text{q}}) + \cdots \right\} + \left\{ \frac{1}{2} (\text{Ap}^2\bar{\text{p}} + \text{A}\bar{\text{p}}\bar{\text{p}}^2) + \cdots \right\} \\ + \left\{ \frac{1}{2} (\text{Ap}^2\text{q} + \text{A}\bar{\text{p}}^2\bar{\text{q}}) + \cdots \right\} + \left\{ \frac{1}{2} (\text{p}^2\bar{\text{p}}\text{q} + \text{p}\bar{\text{p}}^2\bar{\text{q}}) + \cdots \right\} \\ + \left\{ \frac{1}{2} (\text{p}^2\text{q}\bar{\text{q}} + \bar{\text{p}}^2\bar{\text{q}}\bar{\text{q}}) + \cdots \right\} + \left\{ \frac{1}{2} (\text{p}^2\text{qr} + \bar{\text{p}}^2\bar{\text{q}}\bar{\text{r}}) + \cdots \right\} \quad (49)$$

$$f_{c_{\hat{\sigma}}} \stackrel{\text{I}}{=} \{ \text{p}\bar{\text{p}}\text{q}\bar{\text{q}} + \text{p}\bar{\text{p}}\bar{\text{r}}\bar{\text{r}} + \cdots \} \quad (50)$$

$$f_{c_s} \stackrel{\text{V}}{=} \{ \text{ABp}\bar{\text{p}} + \text{ABq}\bar{\text{q}} + \cdots \} \quad (51)$$

$$f_{c_{\hat{i}}} \stackrel{\text{I}}{=} \text{ABXY} \quad (52)$$

(omitted)

The term $1/2(\text{ABp}^2 + \text{AB}\bar{\text{p}}^2)$ in $f_{c_{\bar{\sigma}}}$ (Eq. 49) indicates that the quadruplet of *RS* stereoisomers shown in the type-II stereoisogram (Figure 16) is counted once under the *RS*-stereoisomeric group $\mathbf{T}_{d\bar{\sigma}\hat{i}}$. Note that this quadruplet contains one pair of enantiomers **57** and **57**. Compare this enumeration with the term $1/2(\text{ABp}^2 + \text{AB}\bar{\text{p}}^2)$ in f_{c_s} (Eq. 26) obtained under the point group \mathbf{T}_d . See also the enumeration under the point group \mathbf{T}_d (Figure 14(a)) and the enumeration under the permutation group $\mathbf{S}^{[4]}$ (Figure 14(b)).

The term $\text{ABp}\bar{\text{p}}$ in f_{c_s} (Eq. 51) indicates that the quadruplet of *RS*-stereoisomers shown in the type-V stereoisogram (Figure 17) is counted once under the *RS*-stereoisomeric group $\mathbf{T}_{d\bar{\sigma}\hat{i}}$. Compare this enumeration with the term $2\text{ABp}\bar{\text{p}}$ in f_{c_s} (Eq. 28) obtained

under the point group T_d . Note that the quadruplet of Figure 17 contains two achiral promolecules **48** and **49**. See also the enumeration under the permutation group $S^{[4]}$ (Figure 14(b)), where **48** and **49** are recognized to be a pair of *RS*-diastereomers.

Symmetry-Itemized enumeration of inequivalent quadruplets of *RS*-stereoisomers have been applied to an allene skeleton [205, 206] and an oxirane skeleton [207, 208, 209].

Group hierarchy for stereoskeletons of ligancy 4 has been examined [172], where Fujita's stereoisogram approach is combined with Fujita's proligand method.

Because symmetry-itemized enumerations require mark tables and subduction tables which are not always available, simpler methods are desirable in order to grasp succinct features of *RS*-stereoisomers. As such simpler methods, type-itemized enumerations of quadruplets of *RS*-stereoisomers have been reported [170, 210]. More systematic methods which combine Fujita's proligand method with Fujita's stereoisogram approach have been recently reported as on-line first articles [211, 212].

5. CONCLUSIONS OF MY HALF-CENTURY JOURNEY

5.1. CREATION OF NEW CONCEPTS

My half-century journey has created several new concepts, which are linked with appropriate diagrammatic expressions: e.g., the concept of ITSs which supports Fujita's ITS approach for discussing organic reactions, the concept of sphericities of orbits which supports Fujita's USCI approach for discussing geometric features of stereochemistry, the concept of sphericities of cycles which supports Fujita's proligand method for discussing gross enumeration and recursive enumeration, and the concept of stereoisograms which supports Fujita's stereoisogram approach for discussing stereoisomeric features of stereochemistry.

As a milestone of my journey, these concepts have been demonstrated comprehensively in my recent book entitled "mathematical stereochemistry" [18], which will provide reliable mathematical foundations for further investigation of stereochemistry.

5.2. INTEGRATION OF VAN'T HOFF'S WAY AND LE BEL'S WAY

Modern stereochemistry suffers from conceptual faults and misleading terminology brought about by the lack of reliable mathematical formulations.

1. The conceptual faults stem from the different ways taken by van't Hoff (asymmetry, stereogenicity) [19, 20] and Le Bel (dissymmetry, chirality) [21, 22] at the beginning of stereochemistry and have been continuous sources of confusion over 140 years.

2. Modern stereochemistry lays stress on van't Hoff's way and treats inconsistent cases due to Le Bel's way as exceptions (e.g., pseudoasymmetry). This course of remedy without reliable mathematical formulations is rather ad hoc so as to bring about the misleading terminology to stereoisomerism, the Cahn-Ingold-Prelog system, the *pro-R/pro-S* system and so on.

Fujita's USCI approach emphasizes point groups for the purpose of investigating geometrical features of organic compounds, where point groups are definitely distinguished from permutation groups by developing the concept of sphericities. As found in the enumeration of Fujita's USCI approach, the concept of sphericities provides the distinction between Le Bel's way and van't Hoff's way, because the former is related to point groups (dissymmetry, chirality), while the latter is related to permutation groups (asymmetry, stereogenicity).

Fujita's stereoisogram approach integrates point groups and permutation groups to create *RS*-stereoisomeric groups, after permutation groups are restricted to *RS*-permutation groups and after ligand-reflection groups are created as a new category of groups. Stereoisograms have been developed as diagrammatic expressions of *RS*-stereoisomeric groups. A quadruplet of *RS*-stereoisomers in each stereoisogram is *an intermediate concept for mediating between enantiomers and stereoisomers*. Thereby, van't Hoff's way and Le Bel's way are integrated to reach Aufheben, where *the vertical direction of a stereoisogram is concerned with the chiral aspect for supporting Le Bel's way and the horizontal direction of a stereoisogram is concerned with the RS-stereogenic aspect for supporting van't Hoff's way*. The key for the Aufheben is the diagonal direction of a stereoisogram for characterizing the scleral aspect, which has been hidden behind the confusion over 140 years in modern stereochemistry. As a result, the concept of *RS*-stereoisomers based on stereoisograms provides us with rational theoretical foundations for remedying the conceptual faults and misleading terminology of modern stereochemistry.

5.3. PARADIGM SHIFT PROVIDED BY FUJITA'S STEREOISOGRAM APPROACH

The concept of *RS*-stereoisomers as an intermediate concept brings about a paradigm shift, so that modern stereochemistry will be restructured substantially on the basis of mathematical formulations. This fact is parallel to the historical event that Avogadro's theory has brought about a paradigm shift in chemistry by creating the intermediate concept of *molecule* (e.g., H₂O), which mediates between atoms (e.g., hydrogen atoms and oxygen atoms) and substances (e.g., water). This means that classical descriptions of textbooks on organic chemistry and on stereochemistry should be thoroughly revised in conceptually deeper levels, but not in superficial verbal levels.

REFERENCES

1. H. Nozaki, S. Fujita, H. Takaya, and R. Noyori, Photochemical reaction of ethyl azidoformate with cyclic ethers and acetals, *Tetrahedron* **23** (1967) 45–49.
2. H. Nozaki, H. Takaya, S. Moriuchi, and R. Noyori, Homogeneous catalysis in the decomposition of diazo compounds by copper chelates: Asymmetric carbenoid reactions, *Tetrahedron* **24** (1968) 3655–3669.
3. R. Noyori. Asymmetric catalysis: Science and opportunities (Nobel lecture, December 8, 2001); <http://www.nobelprize.org/nobelprizes/chemistry/laureates/2001/noyorilecture.html>.
4. S. Fujita, *Organic Chemistry of Photography*, Springer-Verlag, Berlin-Heidelberg, 2004.
5. S. Fujita, *Computer-Oriented Representation of Organic Reactions*, Yoshioka-Shoten, Kyoto, 2001.
6. S. Fujita, *Symmetry and Combinatorial Enumeration in Chemistry*, Springer-Verlag, Berlin-Heidelberg, 1991.
7. S. Fujita, *Diagrammatical Approach to Molecular Symmetry and Enumeration of Stereoisomers*, University of Kragujevac, Faculty of Science, Kragujevac, 2007.
8. G. Pólya and R. C. Read, *Combinatorial Enumeration of Groups, Graphs, and Chemical Compounds*, Springer-Verlag, New York, 1987.
9. S. Fujita, *Combinatorial Enumeration of Graphs, Three-Dimensional Structures, and Chemical Compounds*, University of Kragujevac, Faculty of Science, Kragujevac, 2013.
10. S. Fujita, Stereogenicity revisited. Proposal of holantimers for comprehending the relationship between stereogenicity and chirality, *J. Org. Chem.* **69** (2004) 3158–3165.
11. S. Fujita, Integrated discussion on stereogenicity and chirality for restructuring stereochemistry, *J. Math. Chem.* **35** (2004) 265–287.
12. S. Fujita, Pseudoasymmetry, stereogenicity, and the *RS*-nomenclature comprehended by the concepts of holantimers and stereoisograms, *Tetrahedron* **60** (2004) 11629–11638.
13. S. Fujita, Stereoisograms for reorganizing the theoretical foundations of stereochemistry and stereoisomerism: I. Diagrammatic representations of *RS*-stereoisomeric groups for integrating point groups and *RS*-permutation groups, *Tetrahedron: Asymmetry* **25** (2014) 1153–1168.
14. S. Fujita, Stereoisograms for reorganizing the theoretical foundations of stereochemistry and stereoisomerism: II. Rational avoidance of misleading

- standpoints for *R/S*-stereodescriptors of the Cahn-Ingold-Prelog system, *Tetrahedron: Asymmetry* **25** (2014) 1169–1189.
15. S. Fujita, Stereoisograms for reorganizing the theoretical foundations of stereochemistry and stereoisomerism: III. Rational avoidance of misleading standpoints for *Pro-R/Pro-S*-descriptors, *Tetrahedron: Asymmetry* **25** (2014) 1190–1204.
16. R. S. Cahn, C. K. Ingold, and V. Prelog, Specification of molecular chirality, *Angew. Chem. Int. Ed. Eng.* **5** (1966) 385–415.
17. V. Prelog and G. Helmchen, Basic principles of the CIP-system and proposal for a revision, *Angew. Chem. Int. Ed. Eng.* **21** (1982) 567–583.
18. S. Fujita, *Mathematical Stereochemistry*, De Gruyter, Berlin, 2015.
19. J. H. van't Hoff, *La Chimie Dans L'Espace*, P. M. Bazendijk, Rotterdam, 1875.
20. J. H. van't Hoff, *Die Lagerung der Atome im Raume*, (German Translation by F. Herrmann), Friedrich Vieweg und Sohn, Braunschweig, 1877.
21. J. A. Le Bel, Sur les relations qui existent entre les formules atomiques des corps organiqueet le pouvoir rotatoire de leurs dissolutions, *Bull. Soc. Chim. Fr. (2)* **22** (1874) 337–347.
22. J. A. Le Bel, On the Relations Which Exist Between the Atomic Formulas of Organic Compounds and the Rotatory Power of Their Solutions, In *Classics in the Theory of Chemical Combination (Classics of Science, Vol. I)*; O. T. Benfey, Ed., Dover: New York, 1963; pp 161–171.
23. H. Nozaki, Y. Okuyama, and S. Fujita, Addition of carbethoxynitrene to *trans*- and *cis*-propenylbenzene, *Can. J. Chem.* **46** (1968) 3332–3336.
24. S. Fujita and H. Nozaki, Reactions of nitrenes (in Japanese), In *Reactive Intermediates (I) (Hannosei Chukantai in Japanese)*; K. Ichikawa, T. Saegusa, H. Tsubomura, H. Nozaki, and I. Moria, Eds., Kagaku Dojin: Kyoto, 1971; Chapter 5, pp 107–136.
25. S. Fujita, Nitrenes (in Japanese), In *Carbenes, Ylides, Nitrenes, and Benzyne*s; T. Goto, Ed., Hirokawa: Tokyo, 1976; Chapter 3, pp 263–339.
26. S. Fujita, T. Hiyama, and H. Nozaki, Steric course in oxidative ring opening of aziridine-1-carboxylates with dimethyl sulfoxide, *Tetrahedron Lett.* (1969) 1677–1678.
27. S. Fujita, T. Hiyama, and H. Nozaki, Oxidative ring-opening of aziridine-1-carboxylates with sulfoxides, *Tetrahedron* **26** (1970) 4347–4352.
28. S. Fujita, K. Imamura, and H. Nozaki, The absolute configuration of 2-phenylaziridine and its derivatives, *Bull. Chem. Soc. Jpn.* **44** (1971) 1975–1977.
29. H. Nozaki, S. Fujita, and T. Mori, [7](2,6)Pyridinophane and [7](2,6)pyrylophanium perchlorate, *Bull. Chem. Soc. Jpn.* **42** (1969) 1163.

30. S. Fujita and H. Nozaki, Synthesis and conformational studies of [7](2,6)pyridinophanes, *Bull. Chem. Soc. Jpn.* **44** (1971) 2827–2833.
31. S. Fujita and H. Nozaki, Heterophanes. syntheses and structures (review), *Yuki Gosei Kagaku Kyokai-Shi/J. Synth. Org. Chem. Jpn.* **30** (1972) 679–693.
32. S. Fujita, S. Hirano, and H. Nozaki, [7]Metacyclophane and its 13-bromo derivative, *Tetrahedron Lett.* (1972) 403–406.
33. S. Hirano, T. Hiyama, S. Fujita, and H. Nozaki, [6]Metacyclophane and the related compounds, *Chem. Lett.* (1972) 707–708.
34. S. Hirano, H. Hara, T. Hiyama, S. Fujita, and H. Nozaki, Synthetic and structural studies of [6]-, [7]-, and [10]metacyclophanes, *Tetrahedron* **31** (1975) 2219–2227.
35. S. Fujita, Organic compounds for instant photography, *Yuki Gosei Kagaku Kyokai-Shi/J. Synth. Org. Chem. Jpn.* **39** (1981) 331–344.
36. S. Fujita, Image-providing compounds for instant color photography. Their syntheses and characteristics as functionalized dyes, *Yuki Gosei Kagaku Kyokai-Shi/J. Synth. Org. Chem. Jpn.* **40** (1982) 176–187.
37. S. Fujita, Regiospecific attack of methoxide ion on 4-alkoxy-o-quinone imines. a novel route to p-quinone monoacetals, *J. Chem. Soc., Chem. Commun.* (1981) 425–426.
38. S. Fujita, Synthesis and reactions of o-benzoquinone monosulfonimides, *J. Org. Chem.* **48** (1983) 177–183.
39. S. Fujita, K. Koyama, Y. Inagaki, and K. Waki, US Patent 4336322, 1982; Color Photographic Light-Sensitive Material.
40. S. Fujita, H. Hayashi, Y. Y. Shigetoshi Ono, and T. Harada, US Patent 4268625, 1981; Photographic Light-Sensitive Element for the Color Diffusion Transfer Process.
41. S. Fujita, K. Koyama, and S. Ono, Dye releasers for instant color photography. Molecular design and synthetic design, *Nippon Kagaku Kai-Shi* (1991) 1–22.
42. S. Fujita, K. Koyama, and S. Ono, Dye releasers for instant color photography, *Rev. Heteroatom Chem.* **7** (1992) 229–267.
43. S. Fujita, T. Harada, and Y. Yoshida, US Patent 4268624, 1981; Photographic Light-Sensitive Sheet for the Color Diffusion Transfer Process.
44. S. Fujita, K. Koyama, and S. Ono, R&D of dye releasers for Fuji instant color system (FOTORAMA), *Nikkakyo Geppo* (11) (1982) 29–39.
45. S. Fujita, R&D of dye releasers for instant color photography: Design, evaluation, and synthesis, In *Organic Synthesis in Japan, Past, Present, and Future*; R. Noyori, Ed., Tokyo Kagaku Dojin: Tokyo, 1992; pp 89–96.
46. S. Fujita, Description of organic reactions based on imaginary transition structures.
1. Introduction of new concepts, *J. Chem. Inf. Comput. Sci.* **26** (1986) 205–212.

47. S. Fujita, Description of organic reactions based on imaginary transition structures. 8. Synthesis space attached by a charge space and three-dimensional imaginary transition structures with charges, *J. Chem. Inf. Comput. Sci.* **27** (1987) 111–115.
48. S. Fujita, Description of organic reactions based on imaginary transition structures. 5. Recombination of reaction strings in a synthesis space and its application to the description of synthetic pathways, *J. Chem. Inf. Comput. Sci.* **26** (1986) 238–242.
49. S. Fujita, Description of organic reactions based on imaginary transition structures. 2. Classification of one-string reactions having an even-membered cyclic reaction graph, *J. Chem. Inf. Comput. Sci.* **26** (1986) 212–223.
50. S. Fujita, Description of organic reactions based on imaginary transition structures. 3. Classification of one-string reactions having an odd-membered cyclic reaction graph, *J. Chem. Inf. Comput. Sci.* **26** (1986) 224–230.
51. S. Fujita, Description of organic reactions based on imaginary transition structures. 6. Classification and enumeration of two-string reactions with one common node, *J. Chem. Inf. Comput. Sci.* **27** (1987) 99–104.
52. S. Fujita, Description of organic reactions based on imaginary transition structures. 7. Classification and enumeration of two-string reactions with two or more common nodes, *J. Chem. Inf. Comput. Sci.* **27** (1987) 104–110.
53. S. Fujita, Description of organic reactions based on imaginary transition structures. 4. Three-nodal and four-nodal subgraphs for a systematic classification of reactions, *J. Chem. Inf. Comput. Sci.* **26** (1986) 231–237.
54. S. Fujita, A novel approach to systematic classification of organic reactions. Hierarchical subgraphs of imaginary transition structures, *J. Chem. Soc. Perkin II* (1988) 597–616.
55. S. Fujita, Description of organic reactions based on imaginary transition structures. 9. Single-access perception of rearrangement reactions, *J. Chem. Inf. Comput. Sci.* **27** (1987) 115–120.
56. S. Fujita, Logical perception of ring-opening, ring-closure, and rearrangement reactions based on imaginary transition structures. Selection of the essential set of essential rings (ESER), *J. Chem. Inf. Comput. Sci.* **28** (1988) 1–9.
57. S. Fujita, A new algorithm for selection of synthetically important rings. The essential set of essentialset of essential rings (ESER) for organic structures, *J. Chem. Inf. Comput. Sci.* **28** (1988) 78–82.
58. S. Fujita, Canonical numbering and coding of imaginary transition structures. A novel approach to the linear coding of individual organic reactions, *J. Chem. Inf. Comput. Sci.* **28** (1988) 128–137.
59. S. Fujita, Canonical numbering and coding of reaction-center graphs and reduced reaction-center graphs abstracted from imaginary transition structures. A novel

- approach to the linear coding of reaction types, *J. Chem. Inf. Comput. Sci.* **28** (1988) 137–142.
60. G. Pólya, Kombinatorische Anzahlbestimmungen für Gruppen, Graphen und chemische Verbindungen, *Acta Math.* **68** (1937) 145–254.
61. S. Fujita, Enumeration of organic reactions by counting substructures of imaginary transition structures. Importance of orbits governed by coset representations, *J. Math. Chem.* **7** (1991) 111–133.
62. S. Fujita, A novel approach to the enumeration of reaction types by counting reactioncenter graphs which appear as the substructures of imaginary transition structures, *Bull. Chem. Soc. Jpn.* **61** (1988) 4189–4206.
63. S. Fujita, The description of organic reactions, *Yuki Gosei Kagaku Kyokai-Shi/J. Synth. Org. Chem. Jpn.* **44** (1986) 354–364.
64. S. Fujita, “Structure-reaction type” paradigm in the conventional methods of describing organic reactions and the concept of imaginary transition structures overcoming this paradigm, *J. Chem. Inf. Comput. Sci.* **27** (1987) 120–126.
65. S. Fujita, Imaginary transition structures. A novel approach to computer-oriented representation of organic reactions, *Yuki Gosei Kagaku Kyokai-Shi/J. Synth. Org. Chem. Jpn.* **47** (1989) 396–412.
66. S. Fujita, Graphic characterization and taxonomy of organic reactions, *J. Chem. Educ.* **67** (1990) 290–293.
67. S. Fujita, S. Hanai, M. Miyakawa, M. Takeuchi, S. Nakayama, and T. Yasuda, The FORTUNITS system for retrieving organic reactions based on imaginary transition structures, In *Computer Aided Innovation of New Materials II, Part 2*; M. Doyama, K. J. M. Tanaka, and R. Yamamoto, Eds., Elsevier: Amsterdam, 1993; pp 967–972.
68. S. Fujita, FORTUNITS—Development of reaction database based on imaginary transition structures, *CICSJ Bulletin* **12** (1994) 9–12.
69. S. Fujita, Typesetting structural formulae with the text formatter TEX/LATEX, *Comput. Chem.* **18** (1994) 109–116.
70. S. Fujita, XYMTEx for drawing chemical structural formulas, *TUGboat* **16** (1) (1995) 80–88.
71. S. Fujita, Size reduction of chemical structural formulas in XYMTEx (version 3.00), *TUGboat* **22** (4) (2001) 285–289.
72. S. Fujita, Development of XYMTEx2PS for PostScript typesetting of chemical documents containing structural formulas, *J. Comput. Chem. Jpn.* **4** (2005) 69–78.
73. S. Fujita, *XYMTEx—Typesetting Chemical Structural Formulas*, Addison-Wesley Japan, Tokyo, 1997.
74. S. Fujita, *XYMTEx: Reliable Tool for Drawing Chemical Structural Formulas*, On-line Manual, <http://xymtex.com/fujitas3/xymtex/xym501/manual/xymtex-manualPS.pdf>, 2013.

75. S. Fujita, N. Tanaka, XYM notations for electronic communication of organic chemical structures, *J. Chem. Inf. Comput. Sci.* **39** (1999) 903–914.
76. S. Fujita, N. Tanaka, XYM markup language (XYMML) for electronic communication of chemical documents containing structural formulas and reaction schemes, *J. Chem. Inf. Comput. Sci.* **39** (1999) 915–927.
77. S. Fujita, N. Tanaka, XYMT_{EX} (version 2.00) as implementation of the XYM notation and XYM markup language, *TUGboat* **21** (1) (2000) 7–14.
78. N. Tanaka, S. Fujita, XYMJava system for world wide web communication of organic chemical structures, *J. Computer Aided Chem.* **3** (2002) 37–47.
79. N. Tanaka, T. Ishimaru, S. Fujita, WWW (world wide web) communication and publishing of structural formulas by XYMML (XYM markup language)", *J. Computer Aided Chem.* **3** (2002) 81–89.
80. S. Fujita, Articles, books, and internet documents with structural formulas drawn by XYMT_{EX} — Writing, submission, publication, and internet communication in chemistry, *Asian J. TEX* **3** (2009) 89–108.
81. S. Fujita, The XYMT_{EX} system for publishing interdisciplinary chemistry/mathematics books, *TUGboat* **34** (3) (2013) 325–328.
82. F. A. Cotton, *Chemical Applications of Group Theory*, Wiley-International, New York, 1971.
83. E. L. Eliel and S. H. Wilen, *Stereochemistry of Organic Compounds*, John Wiley & Sons, New York, 1994.
84. K. Mislow and M. Raban, Stereoisomeric relationships of groups in molecules, *Top. Stereochem.* **1** (1967) 1–38.
85. H. Hirschmann, Stereoheterotopism and prochirality, *Trans. N. Y. Acad. Sci. Ser. II* **41** (1983) 61–69.
86. S. Fujita, Sphericity governs both stereochemistry in a molecule and stereoisomerism among molecules, *Chem. Rec.* **2** (2002) 164–176.
87. S. Fujita, Sphericity beyond topicity in characterizing stereochemical phenomena. Novel concepts based on coset representations and their subductions, *Bull. Chem. Soc. Jpn.* **75** (2002) 1863–1883.
88. S. Fujita, Promolecules for characterizing stereochemical relationships in non-rigid molecules, *Tetrahedron* **47** (1991) 31–46.
89. S. Fujita, Chirality fittingness of an orbit governed by a coset representation. Integration of point-group and permutation-group theories to treat local chirality and prochirality, *J. Am. Chem. Soc.* **112** (1990) 3390–3397.
90. S. Fujita, Enantiomeric and diastereomeric relationships of ethylene derivatives. Restructuring stereochemistry by a group-theoretical and combinatorial approach, *J. Math. Chem.* **32** (2002) 1–17.

91. S. Fujita, Systematic classification of molecular symmetry by subductions of coset representations, *Bull. Chem. Soc. Jpn.* **63** (1990) 315–327.
92. S. Fujita, Subduction of coset representations. An application to enumeration of chemical structures, *Theor. Chim. Acta* **76** (1989) 247–268.
93. S. Fujita, Stereochemistry and stereoisomerism characterized by the sphericity concept, *Bull. Chem. Soc. Jpn.* **74** (2001) 1585–1603.
94. S. Fujita, Point groups based on methane and adamantane (T_d) skeletons, *J. Chem. Educ.* **63** (1986) 744–746.
95. S. Fujita, Subductive and inductive derivation for designing molecules of high symmetry, *J. Chem. Inf. Comput. Sci.* **31** (1991) 540–546.
96. S. Fujita, Systematic design of chiral molecules of high symmetry. Achiral skeletons substituted with chiral ligands, *Bull. Chem. Soc. Jpn.* **73** (2000) 2679–2685.
97. S. Fujita, Desymmetrization of achiral skeletons by mono-substitution. Its characterization by subduction of coset representations, *Bull. Chem. Soc. Jpn.* **74** (2001) 1015–1020.
98. S. Fujita, Chirality and stereogenicity for square-planar complexes, *Helv. Chim. Acta* **85** (2002) 2440–2457.
99. S. Fujita, The SCR notation for systematic classification of molecular symmetries, *Memoirs of the Faculty of Engineering and Design, Kyoto Institute of Technology* **47** (1999) 111–126.
100. S. Fujita, Theoretical foundation of prochirality. Chirogenic sites in an enantiospheric orbit, *Bull. Chem. Soc. Jpn.* **64** (1991) 3313–3323.
101. S. Fujita, Characterization of prochirality and classification of meso-compounds by means of the concept of size-invariant subductions, *Bull. Chem. Soc. Jpn.* **73** (2000) 2009–2016.
102. S. Fujita, Systematic characterization of prochirality, prostereogenicity, and stereogenicity by means of the sphericity concept, *Tetrahedron* **56** (2000) 735–740.
103. S. Fujita, Chiral replacement criterion for characterizing holotopic and hemitopic relationships, *Bull. Chem. Soc. Jpn.* **73** (2000) 1979–1986.
104. S. Fujita, Prochirality revisited. An approach for restructuring stereochemistry by novel terminology, *J. Org. Chem.* **67** (2002) 6055–6063.
105. S. Fujita, A novel way for understanding the desymmetrization of the tetrahedron in introductory courses of organic stereochemistry (Part I). Importance of orbits and sphericity indices, *Chem. Educ. J.* **8** (2005) Registration No. 8–8.
106. S. Fujita, A novel way for understanding the desymmetrization of the tetrahedron in introductory courses of organic stereochemistry (Part II). Importance of local symmetries appearing in subductions of coset representations, *Chem. Educ. J.* **8** (2005) Registration No. 8–9.

107. S. Fujita, Systematic enumeration of high symmetry molecules by means of unit subduced cycle indices with and without chirality fittingness, *Bull. Chem. Soc. Jpn.* **63** (1990) 203–215.
108. S. Fujita, Soccerane derivatives of given symmetries. Systematic enumeration by means of unit subduced cycle indices, *Bull. Chem. Soc. Jpn.* **64** (1991) 3215–3223.
109. S. Fujita, Unit subduced cycle indices and the superposition theorem. Derivation of a new theorem and its application to enumeration of compounds based on a D_{2d} skeleton, *Bull. Chem. Soc. Jpn.* **63** (1990) 2770–2775.
110. S. Fujita, The USCI approach and elementary superposition for combinatorial enumeration, *Theor. Chim. Acta* **82** (1992) 473–498.
111. S. Fujita, Systematic enumerations of highly symmetric cage-shaped molecules by unit subduced cycle indices, *Bull. Chem. Soc. Jpn.* **62** (1989) 3771–3778.
112. S. Fujita, Adamantane isomers with given symmetries. Systematic enumeration by unit subduced cycle indices, *Tetrahedron* **46** (1990) 365–382.
113. S. Fujita, Enumeration of non-rigid molecules by means of unit subduced cycle indices, *Theor. Chim. Acta* **77** (1990) 307–321.
114. S. Fujita, Systematic enumerations of compounds derived from D_{3h} skeletons. An application of unit subduced cycle indices, *Bull. Chem. Soc. Jpn.* **63** (1990) 1876–1883.
115. S. Fujita, Unit subduced cycle indices with and without chirality fittingness for I_h group. An application to systematic enumeration of dodecahedrane derivatives, *Bull. Chem. Soc. Jpn.* **63** (1990) 2759–2769.
116. S. Fujita, Subsymmetry-itemized enumeration of flexible cyclohexane derivatives, *Bull. Chem. Soc. Jpn.* **67** (1994) 2935–2948.
117. S. Fujita, Benzene derivatives with achiral and chiral substituents and relevant derivatives derived from D_{6h} -skeletons. Symmetry-itemized enumeration and symmetry characterization by the unit-subduced-cycle-index approach, *J. Chem. Inf. Comput. Sci.* **39** (1999) 151–163.
118. S. Fujita, Systematic enumeration of ferrocene derivatives by unit-subduced-cycle-index method and characteristic-monomial method, *Bull. Chem. Soc. Jpn.* **72** (1999) 2409–2416.
119. S. Fujita, Combinatorial enumeration of non-rigid isomers with given ligand symmetries on the basis of promolecules with a symmetry of $D_{\infty h}$, *J. Chem. Inf. Comput. Sci.* **40** (2000) 426–437.
120. S. Fujita, Promolecules with a subsymmetry of O_h . Combinatorial enumeration and stereochemical properties, *Polyhedron* **12** (1993) 95–110.
121. S. Fujita and N. Matsubara, Edge configurations on a regular octahedron. Their exhaustive enumeration and examination with respect to edge numbers and point-

- group symmetries, *Internet Electronic Journal of Molecular Design* **2** (2003) 224–241.
122. S. Fujita, Symmetry-itemized enumeration of cubane derivatives as three-dimensional entities by the fixed-point matrix method of the USCI approach, *Bull. Chem. Soc. Jpn.* **84** (2011) 1192–1207.
123. S. Fujita, Symmetry-itemized enumeration of cubane derivatives as three-dimensional entities by the partial-cycle-index method of the USCI approach, *Bull. Chem. Soc. Jpn.* **85** (2012) 793–810.
124. S. Fujita, Orbits in a molecule. A novel way of stereochemistry through the concepts of coset representations and sphericities (Part 1), *MATCH Commun. Math. Comput. Chem.* **54** (2005) 251–300.
125. S. Fujita, Orbits among molecules. A novel way of stereochemistry through the concepts of coset representations and sphericities (Part 2), *MATCH Commun. Math. Comput. Chem.* **55** (2006) 5–38.
126. S. Fujita, Combinatorial enumeration of stereoisomers by linking orbits in molecules with orbits among molecules. A novel way of stereochemistry through the concepts of coset representations and sphericities (Part 3), *MATCH Commun. Math. Comput. Chem.* **55** (2006) 237–270.
127. S. Fujita, Group-theoretical foundations for the concept of mandalas as diagrammatical expressions for characterizing symmetries of stereoisomers, *J. Math. Chem.* **42** (2007) 481–534.
128. S. Fujita, Mandalas and Fujita's proligand method. A novel way of stereochemistry through the concepts of coset representations and sphericities (Part 4), *MATCH Commun. Math. Comput. Chem.* **57** (2007) 5–48.
129. S. Fujita, The restricted-subduced-cycle-index (RSCI) method for symmetry-itemized enumeration of Kekulé structures and its application to fullerene C₆₀, *Bull. Chem. Soc. Jpn.* **85** (2012) 282–304.
130. S. Fujita, The restricted-subduced-cycle-index (RSCI) method for counting matchings of graphs and its application to Z-counting polynomials and the Hosoya index as well as to matching polynomials., *Bull. Chem. Soc. Jpn.* **85** (2012) 439–449.
131. S. Fujita, Restricted enumerations by the unit-subduced-cycle-index (USCI) approach. IV. The restricted-subduced-cycle-index (RSCI) method for enumeration of Kekulé structures and or perfect matchings of graphs, *MATCH Commun. Math. Comput. Chem.* **69** (2013) 333–354.
132. S. Fujita, Enumeration of three-dimensional structures derived from a dodecahedrane skeleton under a restriction condition. I. The restricted-fixed-point-matrix (RFPM) method based on restricted subduced cycle indices, *J. Comput. Chem. Jpn.* **11** (2012) 131–139.

133. S. Fujita, Enumeration of three-dimensional structures derived from a dodecahedrane skeleton under a restriction condition. II. The restricted-partial-cycle-index (RPCI) method based on restricted subduced cycle indices, *J. Comput. Chem. Jpn.* **11** (2012) 140–148.
134. S. Fujita, Restricted enumerations by the unit-subduced-cycle-index (USCI) approach. I. Factorization of subduced cycle indices, *MATCH Commun. Math. Comput. Chem.* **69** (2013) 263–290.
135. S. Fujita, Restricted enumerations by the unit-subduced-cycle-index (USCI) approach. II. Restricted subduced cycle indices for treating interaction between two or more orbits, *MATCH Commun. Math. Comput. Chem.* **69** (2013) 291–310.
136. S. Fujita, Restricted enumerations by the unit-subduced-cycle-index (USCI) approach. III. The restricted-partial-cycle-index (RPCI) method for treating interaction between two or more orbits, *MATCH Commun. Math. Comput. Chem.* **69** (2013) 311–332.
137. S. Fujita, Graphs to chemical structures 1. Sphericity indices of cycles for stereochemical extension of Pólya's theorem, *Theor. Chem. Acc.* **113** (2005) 73–79.
138. S. Fujita, Graphs to chemical structures 2. Extended sphericity indices of cycles for stereochemical extension of Pólya's coronas, *Theor. Chem. Acc.* **113** (2005) 80–86.
139. S. Fujita, Graphs to chemical structures 3. General theorems with the use of different sets of sphericity indices for combinatorial enumeration of nonrigid stereoisomers, *Theor. Chem. Acc.* **115** (2006) 37–53.
140. S. Fujita, Sphericities of cycles. What Pólya's theorem is deficient in for stereoisomer enumeration, *Croat. Chem. Acta* **79** (2006) 411–427.
141. S. Fujita, Graphs to chemical structures 4. Combinatorial enumeration of planted threedimensional trees as stereochemical models of monosubstituted alkanes, *Theor. Chem. Acc.* **117** (2007) 353–370.
142. S. Fujita, Numbers of monosubstituted alkanes as stereoisomers, *J. Comput. Chem. Jpn.* **6** (2007) 59–72.
143. S. Fujita, Graphs to chemical structures 5. Combinatorial enumeration of centroidal and bicentroidal three-dimensional trees as stereochemical models of alkanes, *Theor. Chem. Acc.* **117** (2007) 339–351.
144. S. Fujita, Enumeration of alkanes as stereoisomers, *MATCH Commun. Math. Comput. Chem.* **57** (2007) 265–298.
145. S. Fujita, Alkanes as stereoisomers. Enumeration by the combination of two dichotomies for three-dimensional trees, *MATCH Commun. Math. Comput. Chem.* **57** (2007) 299–340.
146. S. Fujita, Enumeration of primary, secondary, and tertiary monosubstituted alkanes as stereoisomers, *J. Comput. Chem. Jpn.* **6** (2007) 73–90.

147. S. Fujita, Combinatorial enumeration of three-dimensional trees as stereochemical models of alkanes. An approach based on Fujita's proligand method and dual recognition as uninuclear and binuclear promolecules., *J. Math. Chem.* **43** (2008) 141–201.
148. S. Fujita, Numbers of achiral and chiral monosubstituted alkanes having a given carbon content and given numbers of asymmetric and pseudoasymmetric centers, *Bull. Chem. Soc. Jpn.* **81** (2008) 193–219.
149. S. Fujita, Numbers of asymmetric and pseudoasymmetric centers in enumeration of achiral and chiral alkanes of given carbon contents, *MATCH Commun. Math. Comput. Chem.* **59** (2008) 509–554.
150. S. Fujita, Effect of internal branching on numbers of monosubstituted alkanes as three-dimensional structures and as graphs, *Bull. Chem. Soc. Jpn.* **81** (2008) 1078–1093.
151. S. Fujita, Categorization and enumeration of achiral and chiral alkanes of a given carbon content by considering internal branching, *Bull. Chem. Soc. Jpn.* **81** (2008) 1423–1453.
152. S. Fujita, Systematic comparison between three-dimensional structures and graphs (Part 1). The fate of asymmetry and pseudoasymmetry in the enumeration of monosubstituted alkanes, *MATCH Commun. Math. Comput. Chem.* **62** (2009) 23–64.
153. S. Fujita, Systematic comparison between three-dimensional structures and graphs (Part 2). The fate of asymmetry and pseudoasymmetry in the enumeration of alkanes, *MATCH Commun. Math. Comput. Chem.* **62** (2009) 65–104.
154. S. Fujita, Numbers of alkanes and monosubstituted alkanes. A long-standing interdisciplinary problem over 130 years, *Bull. Chem. Soc. Jpn.* **83** (2010) 1–18.
155. S. Fujita, Dominant representations and a markaracter table for a group of finite order, *Theor. Chim. Acta* **91** (1995) 291–314.
156. S. Fujita, Subduction of dominant representations for combinatorial enumeration, *Theor. Chim. Acta* **91** (1995) 315–332.
157. S. Fujita, Subduction of Q-conjugacy representations and characteristic monomials for combinatorial enumeration, *Theor. Chem. Acc.* **99** (1998) 224–230.
158. S. Fujita, Markaracter tables and Q-conjugacy character tables for cyclic subgroups. An application to combinatorial enumeration, *Bull. Chem. Soc. Jpn.* **71** (1998) 1587–1596.
159. S. Fujita, Direct subduction of Q-conjugacy representations to give characteristic monomials for combinatorial enumeration, *Theor. Chem. Acc.* **99** (1998) 404–410.
160. S. Fujita, Characteristic monomial tables for enumeration of achiral and chiral isomers, *Bull. Chem. Soc. Jpn.* **72** (1999) 13–20.

161. S. Fujita, Characteristic monomials with chirality fittingness for combinatorial enumeration of isomers with chiral and achiral ligands, *J. Chem. Inf. Comput. Sci.* **40** (2000) 1101–1112.
162. S. Fujita, The unit-subduced-cycle-index methods and the characteristic-monomial method. Their relationship as group-theoretical tools for chemical combinatorics, *J. Math. Chem.* **30** (2001) 249–270.
163. S. Fujita, Combinatorial enumeration of cubane derivatives as three-dimensional entities. IV. Gross enumeration by the extended superposition method, *MATCH Commun. Math. Comput. Chem.* **67** (2012) 669–686.
164. S. Fujita, Combinatorial enumeration of cubane derivatives as three-dimensional entities. V. Gross enumeration by the double coset representation method, *MATCH Commun. Math. Comput. Chem.* **67** (2012) 687–712.
165. S. Fujita, Combinatorial enumeration of cubane derivatives as three-dimensional entities. I. Gross enumeration by the proligand method, *MATCH Commun. Math. Comput. Chem.* **67** (2012) 5–24.
166. S. Fujita, Combinatorial enumeration of cubane derivatives as three-dimensional entities. II. Gross enumeration by the markaracter method, *MATCH Commun. Math. Comput. Chem.* **67** (2012) 25–54.
167. S. Fujita, Combinatorial enumeration of cubane derivatives as three-dimensional entities. III. Gross enumeration by the characteristic-monomial method *MATCH Commun. Math. Comput. Chem.* **67** (2012) 649–668.
168. K. Mislow and J. Siegel, Stereoisomerism and local chirality, *J. Am. Chem. Soc.* **106** (1984) 3319–3328.
169. I. Ugi, J. Dugundji, R. Kopp, and D. Marquarding, *Perspectives in Theoretical Stereochemistry*, Springer-Verlag, Berlin-Heidelberg, 1984.
170. S. Fujita, Itemized enumeration of quadruplets of *RS*-stereoisomers under the action of *RS*-stereoisomeric groups, *MATCH Commun. Math. Comput. Chem.* **61** (2009) 71–115.
171. S. Fujita, A proof for the existence of five stereogenicity types on the basis of the existence of five types of subgroups of *RS*-stereoisomeric groups. Hierarchy of groups for restructuring stereochemistry (Part 3), *MATCH Commun. Math. Comput. Chem.* **54** (2005) 39–52.
172. S. Fujita, Combinatorial approach to group hierarchy for stereoskeletons of ligancy 4, *J. Math. Chem.* **53** (2015) 1010–1053.
173. S. Fujita, A new scheme for investigating geometric and stereoisomeric features in stereochemistry, *Tetrahedron* **65** (2009) 1581–1592.
174. S. Fujita, Stereoisograms for discussing chirality and stereogenicity of allene derivatives, *Memoirs of the Faculty of Engineering and Design, Kyoto Institute of Technology* **53** (2005) 19–38.

175. S. Fujita, Stereoisograms of trigonal bipyramidal compounds: I. Chirality and *RS*-stereogenicity free from the conventional “chirality” and “stereogenicity”, *J. Math. Chem.* **50** (2012) 1791–1814.
176. S. Fujita, Stereoisograms of trigonal bipyramidal compounds: II. *RS* -Stereogenicity/*RS*-stereoisomerism versus stereogenicity/stereoisomerism, leading to a revised interpretation of Berry’s pseudorotation, *J. Math. Chem.* **50** (2012) 1815–1860.
177. S. Fujita, Importance of the proligand-promolecule model in stereochemistry. I. The unitsubduced-cycle-index (USCI) approach to geometric features of prismane derivatives, *J. Math. Chem.* **50** (2012) 2202–2222.
178. S. Fujita, Importance of the proligand-promolecule model in stereochemistry. II. The stereoisogram approach to stereoisomeric features of prismane derivatives, *J. Math. Chem.* **50** (2012) 2168–2201.
179. S. Fujita, Stereoisograms of octahedral complexes. I. Chirality and *RS*-stereogenicity, *MATCH Commun. Math. Comput. Chem.* **71** (2014) 511–536.
180. S. Fujita, Stereoisograms of octahedral complexes. II. *RS*-stereogenicity vs. stereogenicity as well as *RS*-stereoisomerism vs. stereoisomerism, *MATCH Commun. Math. Comput. Chem.* **71** (2014) 537–574.
181. S. Fujita, Stereoisograms of cubane derivatives, *Bull. Chem. Soc. Jpn.* **88** (2015) 1653–1679.
182. S. Fujita, Correlation diagrams of stereoisograms for characterizing stereoisomers as binuclear and uninuclear promolecules, *MATCH Commun. Math. Comput. Chem.* **63** (2010) 3–24.
183. S. Fujita, Correlation diagrams of stereoisograms for characterizing uninuclear promolecules. A remedy for over-simplified dichotomy in stereochemical terminology, *MATCH Commun. Math. Comput. Chem.* **63** (2010) 25–66.
184. S. Fujita, Correlation diagrams of stereoisograms for characterizing stereoisomers of cyclobutane derivatives, *J. Math. Chem.* **47** (2010) 145–166.
185. S. Fujita, Theory of organic stereoisomerism in harmony with molecular symmetry, *J. Math. Chem.* **49** (2011) 95–162.
186. S. Fujita, Group-theoretical discussion on the *E/Z*-nomenclature for ethylene derivatives. Discrimination between *RS*-stereoisomeric groups and stereoisomeric groups, *J. Chem. Inf. Comput. Sci.* **44** (2004) 1719–1726.
187. The Commission on the Nomenclature of Organic Chemistry of IUPAC, Rules for the nomenclature of organic chemistry. Section E: Stereochemistry (Recommendations 1974), *Pure and App. Chem.* **45** (1976) 11–30.
188. S. Fujita, Stereoisograms for specifying chirality and *RS*-stereogenicity. A versatile tool for avoiding the apparent inconsistency between geometrical features

- and *RS*-nomenclature in stereochemistry, *MATCH Commun. Math. Comput. Chem.* **61** (2009) 11–38.
189. S. Fujita, Three aspects of an absolute configuration on the basis of the stereoisogram approach and revised terminology on related stereochemical concepts, *J. Math. Chem.* **52** (2014) 1514–1534.
190. S. Fujita, *R/S*-Stereodescriptors determined by *RS*-stereogenicity and their chirality faithfulness, *J. Comput. Aided Chem.* **10** (2009) 16–29.
191. S. Fujita, The stereoisogram approach for remedying discontents of stereochemical terminology, *Tetrahedron: Asymmetry* **25** (2014) 1612–1623.
192. S. Fujita, Misleading classification of isomers and stereoisomers in organic chemistry, *Bull. Chem. Soc. Jpn.* **87** (2014) 1367–1378.
193. S. Fujita, Complete settlement of long-standing confusion on the term “prochirality” in stereochemistry. Proposal of pro-*RS*-stereogenicity and integrated treatment with prochirality, *Tetrahedron* **62** (2006) 691–705.
194. S. Fujita, Stereoisograms for reexamining the concept of prochirality, *Yuki Gosei Kagaku Kyokai-Shi/J. Synth. Org. Chem. Jpn.* **66** (2008) 995–1004.
195. K. R. Hanson, Applications of the sequence rule., *J. Am. Chem. Soc.* **88** (1966) 2731–2742.
196. S. Fujita, Prochirality and pro-*RS*-stereogenicity. Stereoisogram approach free from the conventional “prochirality” and “prostereogenicity”, In *Carbon Bonding and Structures. Advances in Physics and Chemistry*; M. V. Putz, Ed., Springer-Verlag: Dordrecht Heidelberg London, 2011; Vol. 5 of *Carbon Materials: Chemistry and Physics* Chapter 10, pp 227–271.
197. S. Fujita, Stereoisograms: A remedy against oversimplified dichotomy between enantiomers and diastereomers in stereochemistry, In *Chemical Information and Computational Challenge in the 21st Century*; M. V. Putz, Ed., Nova: New York, 2012; Chapter 9, pp 223–242.
198. S. Fujita, Substitution criteria based on stereoisograms to determine prochirality and pro-*RS*-stereogenicity, *MATCH Commun. Math. Comput. Chem.* **61** (2009) 39–70.
199. S. Fujita, *Pro-R/pro-S*-Descriptors specified by *RS*-diastereotopic relationships, not by stereoheterotopic relationships, *J. Comput. Aided Chem.* **10** (2009) 76–95.
200. H. Hirschmann and K. R. Hanson, The differentiation of stereoheterotopic groups, *Eur. J. Biochem.* **22** (1971) 301–309.
201. S. Fujita, Extended pseudoasymmetry and geometric prochirality clarifying the scope of the concepts of holantimers and stereoisograms, *Tetrahedron: Asymmetry* **23** (2012) 623–634.
202. S. Fujita, Stereoisograms of octahedral complexes. III. Prochirality, pro-*RS*-stereogenicity, and pro-ortho-stereogenicity free from the conventional

- “prochirality” and “prostereogenicity”, *MATCH Commun. Math. Comput. Chem.* **71** (2014) 575–608.
203. S. Fujita, Symmetry-itemized enumeration of quadruplets of *RS*-stereoisomers: I the fixed-point matrix method of the USCI approach combined with the stereoisogram approach, *J. Math. Chem.* **52** (2014) 508–542.
204. S. Fujita, Symmetry-itemized enumeration of quadruplets of *RS*-stereoisomers: II the partial-cycle-index method of the USCI approach combined with the stereoisogram approach, *J. Math. Chem.* **52** (2014) 543–574.
205. S. Fujita, Symmetry-itemized enumeration of *RS*-stereoisomers of allenes. I. The fixed point matrix method of the USCI approach combined with the stereoisogram approach, *J. Math. Chem.* **52** (2014) 1717–1750.
206. S. Fujita, Symmetry-itemized enumeration of *RS*-stereoisomers of allenes. II. the partialcycle-index method of the USCI approach combined with the stereoisogram approach, *J. Math. Chem.* **52** (2014) 1751–1793.
207. S. Fujita, Stereoisograms for three-membered heterocycles: I. Symmetry-itemized enumeration of oxiranes under an *RS*-stereoisomeric group, *J. Math. Chem.* **53** (2015) 260–304.
208. S. Fujita, Stereoisograms for three-membered heterocycles: II. Chirality, *RS*-stereogenicity, and ortho-stereogenicity on the basis of the proligand-promolecule model, *J. Math. Chem.* **53** (2015) 305–352.
209. S. Fujita, Stereoisograms for three-membered heterocycles: III. *R/S*-Stereodescriptors for characterizing the *RS*-stereogenic aspect of absolute configuration, *J. Math. Chem.* **53** (2015) 353–373.
210. S. Fujita, Combinatorial enumeration of *RS*-stereoisomers itemized by chirality, *RS*-stereogenicity, and sclerality, *MATCH Commun. Math. Comput. Chem.* **58** (2007) 611– 634.
211. S. Fujita, Type-itemized enumeration of quadruplets of *RS*-stereoisomers. I. Cycle indices with chirality fittingness modulated by type-IV quadruplets, *J. Math. Chem.* (2015); DOI 10.1007/s10910-015-0561-z.
212. S. Fujita, Type-itemized enumeration of quadruplets of *RS*-stereoisomers: II. Cycle indices with chirality fittingness modulated by type-V quadruplets, *J. Math. Chem.* (2015); DOI 10.1007/s10910-015-0562-y.